

**2nd Department of Medicine and Cardiology Center, Medical Faculty,
Albert Szent-Györgyi Clinical Center,
University of Szeged**

**Advances in the diagnostics and management of
congenital heart diseases**

Kálmán Havasi MD

PhD thesis

Tutors:

Prof. Attila Nemes MD, PhD, DSc

Prof. Tamás Forster MD, PhD, DSc

2017

Relevant publications

Full papers

- I. Havasi K, Kalapos A, Berek K, Domsik P, Kohári M, Kovács G, Bogáts G, Hartyánszky I, Forster T, Nemes A. Long-term follow-up of patients with transposition of the great arteries following Senning or Mustard operations. Results from the CSONGRAD Registry. *Orv Hetil* 2016; 157: 104-110. **(impact factor: 0.291)**
- II. Nemes A, Havasi K, Domsik P, Kalapos A, Forster T. Evaluation of right atrial dysfunction in patients with corrected tetralogy of Fallot using 3D speckle-tracking echocardiography. Insights from the CSONGRAD Registry and MAGYAR-Path Study. *Herz* 2015; 40: 980-988. **(impact factor: 0.751)**
- III. Havasi K, Domsik P, Kalapos A, McGhie JS, Roos-Hesselink JW, Forster T, Nemes A. Left atrial deformation analysis in patients with corrected tetralogy of Fallot by 3D speckle-tracking echocardiography (from the MAGYAR-Path Study). *Arq Bras Cardiol* 2017; 108: 129-134. **(impact factor: 1.194)**
- IV. Nemes A, Havasi K, Domsik P, Kalapos A, Forster T. Can univentricular heart be associated with "rigid body rotation"? A case from the three-dimensional speckle-tracking echocardiographic MAGYAR-path study. *Hellenic J Cardiol* 2015; 56: 186-188. **(impact factor: 0.94)**
- V. Nemes A, Havasi K, Forster T. "Rigid body rotation" of the left ventricle in hypoplastic right-heart syndrome: a case from the three-dimensional speckle-tracking echocardiographic MAGYAR-Path Study. *Cardiol Young* 2015; 25: 768-772. **(impact factor: 0.825)**

Abstract

- I. Nemes A, Havasi K, Domsik P, Kalapos A, Forster T. Left atrial function in patients with corrected tetralogy of Fallot – a three-dimensional speckle-tracking

echocardiographic study. Eur Heart J Cardiovasc Imaging 2015; 16 (Suppl 2):
ii207

Table of contents

Title page.....	1
Relevant publications	2
Table of contents	4
Abbreviations	5
1. Introduction	7
2. Aims	9
3. Methods.....	10
4. Results	16
4.1. Long-term follow-up of patients with transposition of the great arteries following Senning or Mustard operations	16
4.2. Volumetric and functional evaluation of atria in corrected tetralogy of Fallot.....	22
4.2.1. Detailed evaluation of right atrial dysfunction in patients with corrected tetralogy of Fallot.....	22
4.2.2. Left atrial deformation analysis in patients with corrected tetralogy of Fallot	31
4.3. Detection of left ventricular 'rigid body rotation' in certain congenital heart diseases	35
4.3.1. 'Rigid body rotation' of the left ventricle in hypoplastic right heart syndrome	35
4.3.2. Left ventricular 'rigid body rotation' in a patient with an univentricular heart	38
5. Discussion	40
5.1. Long-term follow-up of patients with transposition of the great arteries following Senning or Mustard operations	40
5.2. Volumetric and functional evaluation of atria in corrected tetralogy of Fallot.....	42
5.2.1. Detailed evaluation of right atrial dysfunction in patients with corrected tetralogy of Fallot.....	42
5.2.2. Left atrial deformation analysis in patients with corrected tetralogy of Fallot	44
5.3. Detection of left ventricular 'rigid body rotation' in certain congenital heart diseases (hypoplastic right heart syndrome and univentricular heart)	46
6. Conclusions (new observations)	47
7. References	
8. Acknowledgements	
Photocopies of essential publications	

Abbreviations

2D – two-dimensional

3D – three-dimensional

3DS – three-dimensional strain

3DSTE – three-dimensional speckle-tracking echocardiography

AP2CH – apical 2-chamber view

AP4CH – apical 4-chamber view

AS – area strain

ASD – atrial septal defect

CS – circumferential strain

CSONGRÁD Registry – Registry for **C(S)ONGenital caRdiAc Disease** patients at the University of Szeged

cTOF – corrected tetralogy of Fallot

EDV – end-diastolic volume

EF – emptying fraction

ESV – end-systolic volume

FAC – fractional area change

LV – left ventricle

HRHS – hypoplastic right heart syndrome

LA – left atrium

LS – longitudinal strain

NCCM – noncompaction cardiomyopathy

MAGYAR-Path Study – **M**otion **A**nalysis of the heart and **G**reat vessels **bY** three-dimension**A**l speckle-t**R**acking echocardiography in **P**athological cases Study

NYHA – New York Heart Association

PDA – persistent ductus arteriosus

RA – right atrium

RBR – rigid body rotation

RS – radial strain

RV – right ventricle

STE – speckle-tracking echocardiography

SV – stroke volume

TAPSE – tricuspid annular plane systolic excursion

TGA – transposition of the great arteries

VAS – visual analogue scale

V_{\max} – maximum atrial volume

V_{\min} – minimum atrial volume

V_{preA} – pre-atrial contraction volume

VSD – ventricular septal defect

1. Introduction

There is an increasing number of young adult patients with different congenital heart diseases in adult cardiology patient care, who were previously treated and followed in paediatric cardiology. However, care of these patients may be challenging for adult cardiologists due to their special late haemodynamic and arrhythmologic consequences (1). Due to absence of evidences, studies are warranted to demonstrate clinical value of certain diagnostic and therapeutic approaches in this special patient population.

(Dextro-) transposition of the great arteries (TGA) is the most frequent cyanotic congenital heart disease, which accounts for 5-7% of all congenital cardiac abnormalities (2). It occurs in approximately 20/100,000 live-birth, typically males are affected in 60-70%. It is rarely associated with other congenital abnormalities and shows multifactorial inheritance regarding the literature (3). In congenital TGA, the aorta arises from the right ventricle (RV), while the pulmonary artery originates from the left ventricle (LV). Accordingly, there are two circulations not communicating with each other, this condition is compatible with life only if there is a connection between them, like in the presence of an atrial septal defect (ASD), ventricular septal defect (VSD), persistent ductus arteriosus (PDA) or their combination (4).

Regarding these facts, treatment of TGA is to perform a palliative operation to keep communication between the two circulations in early infancy, then following weight gain to restore circulation via reconstructive procedures (5, 6). From the 1960s till 1990s, atrial reconstructive switch surgery based on the creation of a flap was the widespread methodology. The most commonly used procedures were the Mustard and Senning operations (7). From the 1990s, these methods have been replaced by the arterial switch surgery, when the origin of the aorta and the pulmonary artery is transected and interchanged, then the pulmonary artery is sutured to the RV, while the aorta is attached to the LV (4).

However, it would be important to know whether there are any differences in survival, complications and quality of life of patients undergoing one of the most commonly used atrial switch surgeries (Senning vs. Mustard procedures) during a long-term follow-up.

Tetralogy of Fallot is one of the most common cyanotic congenital heart disease is occurs in 7 to 10 percent of all congenital heart diseases (1, 2). In the past it was known as “blue baby” syndrome. From the 1940’s it was available to perform some types of palliative

surgeries just like: Blalock-Taussig shunts (it is a connection between the subclavian artery and the pulmonary artery with a tube) or the Potts shunt and Waterstone shunts which are direct connections between the aorta and the pulmonary artery. Some years later after a successful palliative operation total correction became available, when the surgeon closed the ventricular defect, repaired the right ventricular outflow tract. Nowadays, primary direct total correction is the first line treatment option in younger hood.

Nowadays angle-independent speckle-tracking echocardiography (STE) -derived myocardial deformation analysis is one of the main focus of cardiac ultrasound technology (8). Three-dimensional (3D) echocardiography coupled with STE capability is a novel methodology, which has been demonstrated to be useful for the assessment of volumes and functional properties of cardiac chambers (9). 3DSTE allows complex assessment of atrial and ventricular morphological and functional evaluations including volumetric and strain measurements from the same acquired 3D dataset at the same time.

There is increased scientific interest in myocardial deformation analysis in adult patients with corrected tetralogy of Fallot (cTOF) (10-12). Recently, alterations in RV (10, 11) and LV (11) functional properties could be demonstrated by 3DSTE.

However, quantitative detailed right (RA) and left atrial (LA) deformation assessment has never been performed in cTOF patients with 3DSTE.

In addition to volumetric and strain assessments, 3DSTE was also found to be feasible for the non-invasive evaluation of LV *rotational mechanics* (13-15). LV twist is resulted from the movement of two orthogonally oriented muscular bands of a helical myocardial structure with a consequent clockwise rotation of the LV base and counterclockwise rotation of the LV apex (13, 15). However, in some special circumstances, the near absence of LV twist called as LV "rigid body rotation" (RBR) could be detected in some diseases like in different cardiomyopathies (16, 17), infiltrative disorders (18), etc.

However, LV-RBR has never been found in different kinds of congenital heart diseases.

2. Aims

To examine and compare survival, functional grading, arrhythmologic control and long-term quality of life in patients with transposition of the great arteries following Senning and Mustard operations.

To assess three-dimensional speckle tracking echocardiography-derived right atrial volumetric and strain parameters in adult patients with corrected tetralogy of Fallot and to compare data to that of healthy matched controls.

To detect changes in left atrial volumes, volume-based functional properties and strain parameters in corrected tetralogy of Fallot patients as compared to age- and gender matched healthy controls.

To confirm presence of near absence of left ventricular twist called as left ventricular 'rigid body rotation' in certain congenital diseases.

3. Methods

Patient population (general considerations). Since 1962, more than 2,500 patients with different kinds of congenital heart diseases have been treated and/or operated on at the Department of Paediatrics, Department of Heart Surgery and 2nd Department of Medicine and Cardiology Center at the University of Szeged. A registry has been created named after Csongrád County, where the University of Szeged is located. In this registry, all available demographic, clinical and prognostic information related to these patients have been summarized (**CSONGRAD Registry: Registry for C(S)ONGenital caRdiAc Disease** patients at the University of Szeged). Complete two-dimensional (2D) Doppler echocardiography and 3DSTE have been performed in some cases. Results from these measurements were partially summarized in the **MAGYAR-Path Study (Motion Analysis of the heart and Great vessels bY three-dimensionAl speckle-tRacking echocardiography in Pathological cases)**. This has been organized to evaluate usefulness, diagnostic and prognostic value of 3DSTE-derived volumetric, strain, rotational etc. parameters in pathological cases at our center ('magyar' means 'Hungarian' in Hungarian language). Informed consent was obtained from each patient and the study protocol conformed to the ethical guidelines of the 1975 Declaration of Helsinki, as reflected in a prior approval by the institution's human research committee.

Characteristics of the follow-up. Our aim was to contact all patients by phone, mail or other available way. Death was categorized as early or late whether death occurred within 30 days after surgery or not. Patients alive were examined regarding the follow-up time, New York Heart Association (NYHA) heart failure classification, baffle-related complications, known arrhythmias, presence of pacemaker, and quality of life and functional capacity characterized by special questionnaires.

NYHA classification of heart failure. For assessment of the severity of heart failure, the NYHA classification was used introduced for the first time in 1928 (19):

NYHA class I: No limitation in physical activity and ordinary physical activity causes no fatigue, shortness of breath or palpitation.

NYHA class II: Moderately limited physical activity, no resting symptoms, but ordinary physical activity causes fatigue, dyspnoea, palpitations and angina.

NYHA class III: Marked limitation in physical activity, no resting symptoms, but less than ordinary physical activity is able to provoke symptoms detailed above.

NYHA class IV: Resting symptoms, small physical activity is able to augment the above mentioned symptoms.

Arrhythmological follow-up. During the follow-up, we were looking for brady- and tachyarrhythmias associated with haemodynamic failure (atrial fibrillations and flutter, higher grade ventricular arrhythmias or atrio-ventricular blocks, etc.), radiofrequency ablation, pacemaker implantation, etc. in the past medical history.

Featuring quality of life and functional status. Special questionnaires were used for the estimation of quality of life and functional status. It took 8-10 minutes per patient to complete. To assess health condition, the visual analogue scale (VAS), as the part of EuroQol questionnaire was applied, which is a linear scale from 1 to 100, where 1 means the worst, while 100 characterizes the best health condition (20). The so called EQ-5D-5L questionnaire was also filled in by the patients featuring questions about mobility, self-sufficiency, performance of usual activities, pain, malaise, depression and anxiety (21). Results were classified in a scale from 1 to 5: one meant no problem, while five meant severe problem. In addition to the NYHA classification for judgement of functional capacity, ability indices were applied using the Baecke questionnaire containing three parts: physical activity at the workplace, during sports and leisure excluding sport. It was measured whether they have sitting work, or have to walk or lift heavy subjects while working, whether they experience fatigue, sweating or feel that their job is more exhausting compared to their colleagues. When sporting habits were examined, it was asked whether mild, moderate or high intensity sport was played, how often the patient had sporting activities (weekly or monthly), and whether it was more or less frequent compared to others. When leisure activities were examined, it was assessed that how much time was spent on cycling or walking. A total of 18 questions were asked, and all questions were scored from 1 to 5, where one was the lowest and five was the highest activity. Based on these data, work-, sport- and leisure-activity indices were calculated (22).

Two-dimensional Doppler and tissue Doppler echocardiography. Complete two-dimensional (2D) Doppler echocardiographic examinations were performed by a

commercially available Toshiba Artida™ echocardiography equipment (Toshiba Medical Systems, Tokyo, Japan) with a PST-30SBP (1-5 MHz) phased-array transducer. LV and LA dimensions, volumes and ejection fraction were measured by Teichholz method in parasternal long-axis view in all cases (23). Colour Doppler echocardiography was used to visually quantify degree of mitral and tricuspid regurgitations. Following Doppler assessment of E/A, the ratio of transmitral E velocity to early diastolic mitral annular velocity (E') was measured by tissue Doppler echocardiography (23). Tricuspid annular plane systolic excursion (TAPSE) and right ventricular fractional area change (RV-FAC) were also calculated (24).

Three-dimensional speckle tracking echocardiography-derived left/right atrial volumetric measurements. All patients underwent 3D echocardiographic acquisitions immediately following 2D echocardiographic study using a commercially available PST-25SX matrix-array transducer (Toshiba Medical Systems, Tokyo, Japan) with 3DSTE capability (9, 25, 26). Within a single breath-hold and during a constant RR interval, 6 wedge-shaped subvolumes were acquired from an apical window to create full-volume 3D datasets. The sector width was decreased as much as possible to improve temporal and spatial resolution of the image in order to obtain a full-volume 3D dataset of LA/RA with optimal border delineation. Chamber quantification by 3DSTE was performed off-line using 3D Wall Motion Tracking software version 2.5 (Toshiba Medical Systems, Tokyo, Japan). 3D echocardiographic datasets were displayed in apical 4-chamber (AP4CH) and 2-chamber (AP2CH) views and 3 short-axis views in basal, mid-atrial, and superior LA/RA regions, respectively (Figures 1 and 2). In the AP4CH and AP2CH views, the endocardial border was traced by setting multiple reference points by the user starting at base of the LA/RA at mitral/tricuspid valve level advancing toward the lowest point of the LA/RA and excluding the LA/RA appendage and pulmonary/caval veins from the atrial cavity (27-29) (Figures 1 and 2). The epicardial border was adjusted manually or by setting a default thickness for the myocardium. After detection of the LA/RA borders at the end-diastolic reference frame, 3D wall motion tracking, which is based on 3D block-matching algorithm, was automatically performed by the software. The user could correct the shape of the LA/RA if needed throughout the entire cardiac cycle. The following volumetric calculations have been performed for LA/RA respecting the cardiac cycle (Figures 1 and 2):

- (1) maximum volume (V_{\max}) at end-systole, the time at which atrial volume was the largest just before mitral/tricuspid valve opening,
- (2) minimum volume (V_{\min}): at end-diastole, the time at which atrial volume was at its nadir before mitral/tricuspid valve closure,
- (3) volume before atrial contraction (V_{preA}): the last frame before mitral/tricuspid valve reopening or at the time of P wave on the electrocardiogram.

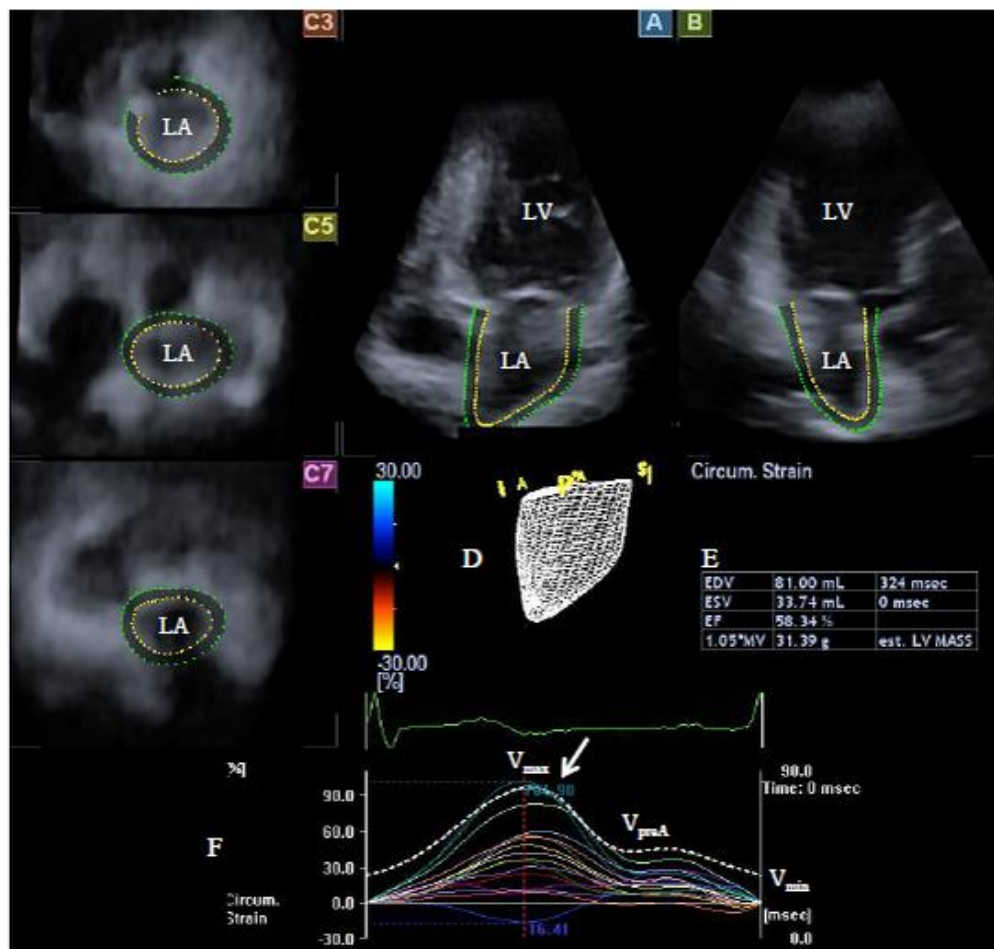


Figure 1. Images from three-dimensional (3D) full-volume dataset showing left atrium (LA) in a patient with corrected tetralogy of Fallot are presented: (A) apical four-chamber view, (B) apical two-chamber view, (C3) short-axis view at basal, (C5) mid- and (C7) superior left atrial level. A 3D cast (D), volumetric data (E), time–global volume and time–segmental strain curves (F) of the LA are also presented. Dashed curve (F) represents LA volume changes during the cardiac cycle with maximum (V_{\max}), minimum (V_{\min}) LA volumes and LA volume at atrial contraction (V_{preA}). White arrow represents peak strain (F).

Abbreviations: LA = left atrium, LV = left ventricle

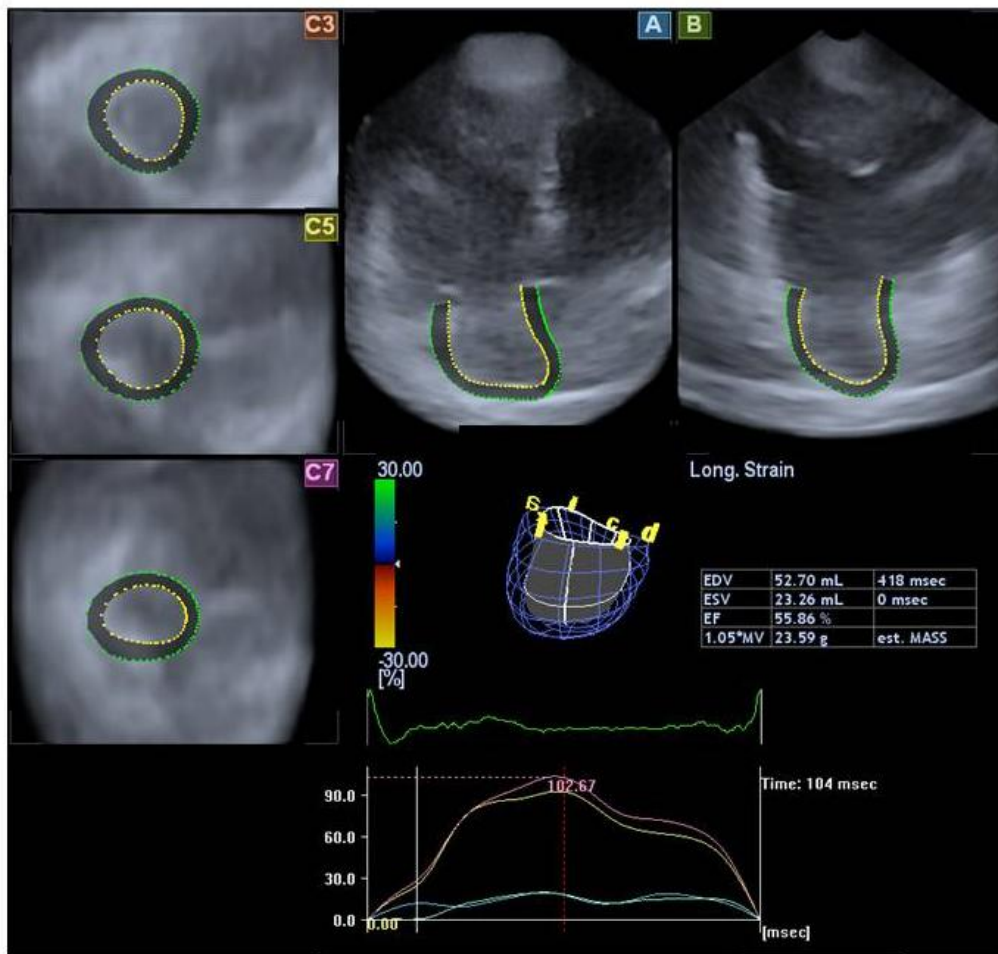


Figure 2. Images from three-dimensional full-volume dataset showing right atrium in a patient with corrected tetralogy of Fallot: (A) apical four-chamber view, (B) apical two-chamber view, (C3) parasternal short-axis view at basal, (C5) mid- and (C7) superior right atrial level. The semi-automated right atrial border definition and three-dimensional “wire” reconstruction of the right atrium based on three-dimensional speckle tracking echocardiographic analysis are also presented.

From the three volumes, several parameters characterizing each phase of LA/RA function could be assessed (Table 1).

Three-dimensional speckle tracking echocardiography-derived left/right atrial strain measurements. The following global, mean segmental and segmental (basal, mid-atrial and superior) peak strains (characterizing atrial reservoir function) and strains at atrial contraction (characterizing atrial active contractile function) are routinely measured by the software in a semi-automatic fashion from the 3D echocardiographic dataset (25, 26) (Figures 1 and 2):

- (1) Longitudinal strain in the direction tangential to the endocardial contour,
- (2) Circumferential strain in circumferential direction,
- (3) Radial strain in perpendicular direction to the endocardial contour,
- (4) 3D strain defined as strain in the direction of wall thickening, and
- (5) Area strain as a ratio of endocardial area change during the cardiac cycle

Table 1. Formulas to calculate atrial stroke volumes and emptying fractions in each phase of left/right atrial motion

Functions	Stroke volumes (ml)	Emptying fractions (%)
Reservoir	$\text{Total SV} = V_{\text{max}} - V_{\text{min}}$	$\text{Total EF} = \frac{\text{Total SV}}{V_{\text{max}}}$
Conduit function	$\text{Passive SV} = V_{\text{max}} - V_{\text{preA}}$	$\text{Passive EF} = \frac{\text{Passive SV}}{V_{\text{max}}}$
Active contraction	$\text{Active SV} = V_{\text{preA}} - V_{\text{min}}$	$\text{Active EF} = \frac{\text{Active SV}}{V_{\text{preA}}}$

Abbreviations: EF = emptying fraction, SV = stroke volume, V_{max} = maximum left/right atrial volume, V_{min} = minimum atrial volume, V_{preA} = atrial volume before atrial contraction

Statistical analysis. All data are reported as mean \pm standard deviation. A value of $p < 0.05$ was considered to be statistically significant. For comparing variables, Student's t -test, chi-square analysis, and Fisher's exact test were used. Pearson's coefficient was used for interobserver and intraobserver correlations. Kaplan–Meier life table estimates of survival were used to summarize the follow-up. Differences in survival rates between groups were tested by the long-rank test. Intra- and interobserver agreements were studied according to Bland and Altman method. MedCalc software was used for statistical calculations (MedCalc, Mariakerke, Belgium).

4. Results

4.1. Long-term follow-up of patients with transposition of the great arteries following Senning or Mustard operations

Patient populations. Regarding the data of the CSONGRAD Registry, from 1961 till 2013, 196 infants with TGA were operated on with "non-arterial switch" technique at the Department of Heart Surgery of the Medical University of Szeged, later Albert Szent-Györgyi Medical University, presently University of Szeged, Faculty of Medicine. Only palliation was performed in 104 out of 196 patients, while in the remaining 92 cases, reconstructive surgery was also performed: Mustard operation in 48 cases, Senning operation in 37 cases, Rastelli operation in 5 cases and other intervention in 2 cases.

The present study comprised 85 TGA patients with Mustard (n = 48) or Senning (n = 37) operation. Clinical data of patients are presented in Table 2. Generally it could be said, that regardless of the type of the procedure, male gender dominated. In two-thirds of the cases, isolated TGA was present relative to the total number of patients and Mustard and Senning operation subgroups. Mean age of Mustard surgery patients proved to be tendentiously higher. It could be explained by the fact that Mustard surgeries were dominantly performed in the 1960-70s, while Senning surgeries in the 1980-90s. Moreover, Mustard surgeries were performed a few decades earlier, when early procedures were carried out in normothermia or in moderate hypothermia. Later, deep hypothermia was used, which allowed total cardiac arrest for a shorter period making the operation easier to perform technically. Moreover, anaesthesiological techniques and possibilities in postoperative treatment also changed a lot. Learning curve of both methodologies could also influence the results. In the first cases of the Mustard group, surgery was performed too late after complications in relatively "old" patients.

Features of follow-up. Success rate of our follow-up proved to be 74% (63 out of 85 cases). Follow-up proved to be more successful in the Senning operated group, which could be explained by the fact that Mustard operation were performed earlier, therefore documentation was less available compared to that of Senning operated patients. Clinical data of follow-up patients are summarized in Table 3. From the Mustard surgery group, two females delivered two healthy babies without any complications. There was no pregnancy in the Senning group.

Table 2. Clinical data of patients

	All TGA patients	Senning operation	Mustard operation	p
Patient number (%)	85 (100)	37 (44)	48 (57)	
Male (%)	69 (81)	33 (89)	36 (75)	0.16
Age at the surgery (years)	2.6 ± 2.6	2.0 ± 2.3	3.0 ± 2.8	0.08
Isolated TGA (%)	56 (66)	24 (65)	32 (67)	1.00
TGA with associated vitium	29 (34)	13 (35)	16 (33)	1.00
TGA with PDA	12 (14)	9 (24)	3 (6)	0.03
TGA with PS	10 (12)	3 (8)	7 (15)	0.50
TGA with ASD	12 (14)	2 (5)	10 (21)	0.06
TGA with VSD	11 (13)	4 (11)	7 (15)	0.75
Ratio of followed patients (%)	63 (74)	31 (84)	32 (67)	0.09

Abbreviations. ASD = atrial septal defect, PDA = persistent ductus arteriosus, PS = pulmonary stenosis, TGA = transposition of the great arteries, VSD = ventricular septal defect

Table 3. Clinical data of followed patients

	TGA patients	Senning operation	Mustard operation	p
Patient number (%)	85 (100)	37 (44)	48 (57)	0.33
Followed patients (%)	63 (74)	31 (84)	32 (67)	0.09
Male (%)	51 (81)	27 (87)	24 (75)	0.34
Age at the surgery (years)	2.7 ± 2.9	2.2 ± 2.4	3.1 ± 3.3	0.22
Duration of follow-up (years)	24.4 ± 8.5	20.3 ± 4.5	29.4 ± 9.7	<0.0001
Mortality (%)	28 (44)	12 (39)	16 (50)	0.45
early (<30 days)	8 (13)	5 (16)	3 (9)	0.47
late (>30 days)	20 (32)	7 (23)	13 (41)	0.18
Baffle-related complications (%)	2 (3)	1 (3)	1 (3)	1.00
Patients alive (%)	35 (56)	19 (61)	16 (50)	0.45
Age in 2015 (years)	30.7 ± 7.6	24.6 ± 2.8	37.9 ± 4.2	<0.0001
Arrhythmia (%)	13 (37)	6 (32)	7 (44)	0.50
Pacemaker (%)	9 (26)	3 (16)	6 (38)	0.25
Patients completed a quality of life questionnaire (%)	25 (40)	16 (52)	9 (28)	0.07
mean NYHA class	1.2 ± 0.4	1.1 ± 0.3	1.3 ± 0.5	0.06
NYHA I (%)	20 (80)	14 (88)	6 (67)	0.31
NYHA II (%)	5 (20)	2 (13)	3 (33)	0.31
NYHA III-IV (%)	0 (0)	0 (0)	0 (0)	1.00

Abbreviations. NYHA = New York Heart Association classification of heart failure, TGA = transposition of the great arteries

Mortality. Twelve out of 31 followed Senning-operated patients died during the follow-up (39%, 0-19 years after operation, mean: 3.5 ± 6.8 years) from which accurate date of death is unknown in two cases. Sixteen out of 32 Mustard-operated patients died (50%, 0-35 years after operation, mean: 5.3 ± 11.2 years), from which date of death is unknown in three subjects (Table 3). Regarding to the survival curves there were no significant differences in mortality between the two patient groups (Figure 3).

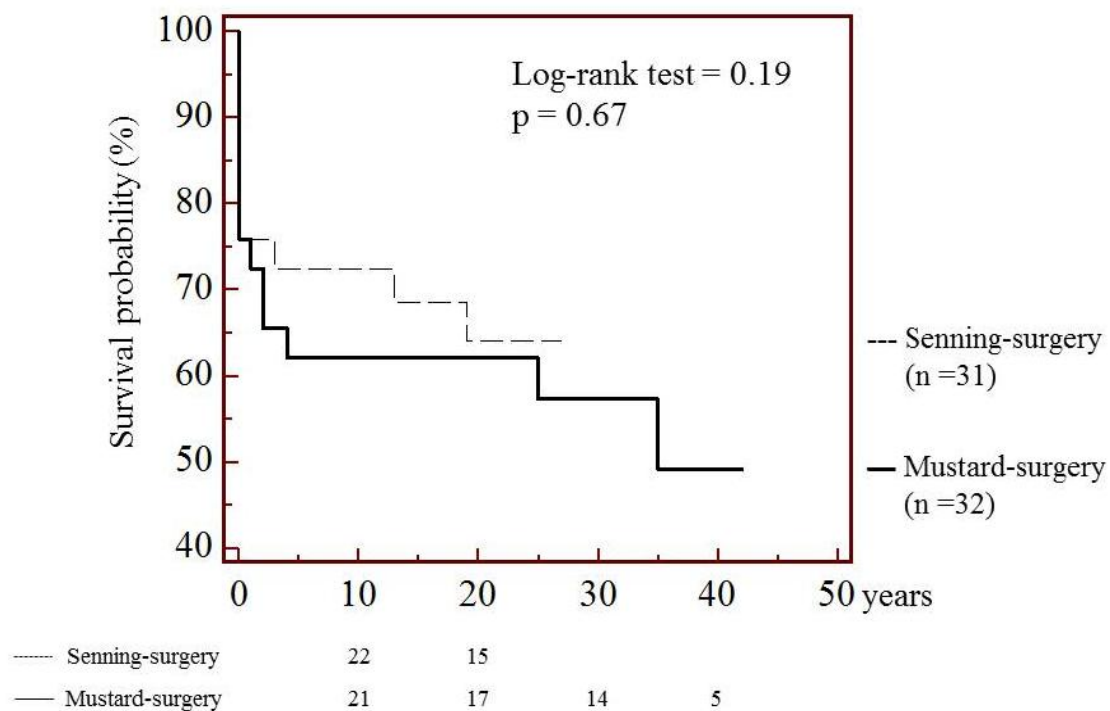


Figure 3. Kaplan-Meier curves demonstrating survival of Mustard and Senning surgery patients

Baffle-related complications. Regarding the results of long-term follow-up it could be said that baffle-related complications had arisen in only a few cases (Table 2). In a Senning operated patient, two years after the surgery, arterial switch operation was required due to baffle leak and multiple kinking and fenestration of the baffle. In a Mustard operated patient, heart failure developed 25 years after the surgery. The patient was reoperated and a new channel was formed from a Dacron-patch replacing the severely calcified baffle. On the 13th postoperative day, the patient died at the intensive care unit.

Heart failure. NYHA classification was used to characterize (the severity of) heart failure. The proportion of respondents is presented in Table 3. Mean NYHA class and frequency of NYHA class II proved to be higher in Mustard operated patients, but the difference did not reach the level of statistical significance. However, limited number of patients was examined and mean age and follow-up time of Mustard operated patients were higher as compared to Senning operated subjects.

Arrhythmology. There were no differences in the frequency of arrhythmia and pacemaker implantation when patient groups were compared (Table 3). Type of arrhythmia was atrial fibrillation or flutter in all cases. Successful radiofrequency ablation was performed three times after Senning operation and four times after Mustard operation. Indication of pacemaker implantation was atrioventricular block or sick sinus syndrome in all cases. To catch arrhythmia substrate, transbaffle puncture was required in some cases.

Quality of life. Higher ratio of Senning surgery patients achieved higher qualification and can perform physical work. Statistical analysis did not find significant differences only tendentious alterations between the groups (Table 4). From other features of quality of life, parameters of VAS, EQ-5D-5L and Baecke-questionnaire proved to be significantly favourable in the Senning operated group, which suggest favourable health condition and functional capacity in these patients at the long-term follow-up.

Table 4. Quality of life data of followed-up patients

	TGA patients	Senning operation	Mustard operation	p
Followed-up patients (%)	63 (100)	31 (49)	32 (51)	0.90
Quality of life questionnaire filled out (%)	25 (40)	16 (52)	9 (28)	0.07
Highest educational attainment				
Elementary school (%)	5 (20)	3 (19)	2 (22)	1.00
Vocational school or High school (%)	8 (32)	5 (31)	3 (33)	1.00
Graduation (%)	9 (36)	7 (44)	2 (22)	0.40
College (%)	2 (8)	1 (6)	1 (11)	1.00
University (%)	1 (4)	0 (0)	1 (11)	1.00
Job				
No job (%)	3 (12)	0 (0)	3 (33)	0.04
Intellectual work (%)	8 (32)	5 (31)	3 (33)	1.00
Light physical work (%)	12 (48)	9 (56)	3 (33)	0.41
Hard physical work (%)	2 (8)	2 (13)	0 (0)	0.52
Health condition (VAS)	75 ± 18	77 ± 20	69 ± 11	0.05
EQ5D5L index	0.8 ± 0.2	0.9 ± 0.1	0.7 ± 0.4	0.009
Baecke-questionnaire				
Sport index	2.5 ± 0.9	2.7 ± 0.9	2.1 ± 0.8	0.007
Leisure index	3.3 ± 0.8	3.5 ± 0.6	3.1 ± 1.0	0.06
Work index	2.3 ± 0.8	2.5 ± 0.8	2.1 ± 0.7	0.04

Abbreviations: VAS = visual analogue scale, TGA = transposition of the great arteries

4.2. Volumetric and functional evaluation of atria in corrected tetralogy of Fallot

4.2.1. Detailed evaluation of right atrial dysfunction in patients with corrected tetralogy of Fallot

Patient population. From the CSONGRÁD Registry, 17 consecutive adult patients with cTOF were chosen to be involved into the present study (Table 5). Patients had undergone isolated tetralogy of Fallot repair at 4.2 ± 2.3 years. Their results were compared to 18 age- and gender-matched healthy controls. All subjects with known diseases were excluded from the control group. Complete 2D Doppler echocardiography and 3DSTE were performed in all cTOF cases and controls.

Table 5. Clinical and two-dimensional echocardiographic data in patients with corrected tetralogy of Fallot and controls

	cTOF patients (n=17)	Controls (n=18)	p-value
Clinical data			
Age (years)	38.2 ± 11.8	36.4 ± 9.8	0.63
Male gender (%)	7 (41)	10 (56)	0.51
Two-dimensional echocardiography			
LA diameter (mm)	41.8 ± 6.60	32.7 ± 3.4	<0.0001
LV end-diastolic diameter (mm)	55.8 ± 20.3	47.4 ± 7.0	0.11
LV end-diastolic volume (ml)	117.2 ± 31.6	96.8 ± 17.1	0.02
LV end-systolic diameter (mm)	33.2 ± 7.3	29.8 ± 4.3	0.10
LV end-systolic volume (ml)	45.3 ± 24.0	33.9 ± 10.9	0.08
Interventricular septum (mm)	9.8 ± 1.5	9.5 ± 2.1	0.64
LV posterior wall (mm)	9.7 ± 1.5	9.5 ± 2.5	0.79
LV ejection fraction (%)	62.3 ± 12.0	65.4 ± 7.1	0.35

Abbreviations: LV = left ventricular, cTOF= corrected tetralogy of Fallot

Two-dimensional echocardiographic data. Clinical and standard 2D echocardiographic data are summarized in Table 5. Significant (\geq grade 2) mitral and tricuspid regurgitations could be detected in 1 (6%) and 6 (35%) cTOF patients, respectively. None of the healthy controls showed significant (\geq grade 2) mitral or tricuspid regurgitation. TAPSE and RV-FAC of cTOF patients proved to be 17.8 ± 4.1 mm and 33.1 ± 4.3 , respectively.

Three-dimensional speckle tracking echocardiography-derived volumes and volume-based functional properties. Significantly increased right atrial volumes respecting the cardiac cycle could be detected in cTOF patients. Total and passive atrial emptying fractions proved to be significantly decreased in patients with cTOF (Table 6).

Table 6. Comparison of 3DSTE-derived volumetric and volume-based functional right atrial parameters in patients with corrected tetralogy of Fallot and controls

	cTOF patients (n=17)	Controls (n=18)	p-value
Calculated volumes (ml)			
Maximum RA volume (V_{\max})	64.9 ± 33.8	37.8 ± 10.1	0.003
Minimum RA volume (V_{\min})	49.8 ± 32.8	23.1 ± 7.9	0.002
RA volume before atrial contraction (V_{preA})	57.9 ± 32.1	30.2 ± 9.0	0.001
Stroke volumes (ml)			
Total atrial SV	15.1 ± 6.4	14.6 ± 4.8	0.79
Passive atrial SV	6.9 ± 4.7	7.5 ± 4.3	0.70
Active SV	8.1 ± 5.1	7.1 ± 3.3	0.49
Emptying fractions (%)			
Total atrial EF	26.4 ± 12.4	39.1 ± 8.8	0.001
Passive atrial EF	11.2 ± 6.8	19.8 ± 9.0	0.003
Active atrial EF	17.3 ± 11.9	23.7 ± 10.3	0.10

Abbreviations: V_{\max} = maximum right atrial volume, V_{\min} = minimum right atrial volume, V_{preA} = right atrial volume before atrial contraction, SV = stroke volume, EF = emptying fraction, cTOF = corrected tetralogy of Fallot, RA = right atrial

Table 7. Comparison of three-dimensional speckle-tracking echocardiography-derived global and segmental peak right atrial strain parameters in patients with corrected tetralogy of Fallot and controls

	cTOF patients (n=17)	Controls (n=18)	p-value
Global strains			
Radial strain (%)	-9.1 ± 5.1	-15.0 ± 10.0	0.05
Circumferential strain (%)	7.5 ± 8.7	12.0 ± 8.4	0.13
Longitudinal strain (%)	17.3 ± 9.2	30.8 ± 11.2	0.0007
3D strain (%)	-4.5 ± 3.7	-6.7 ± 5.6	0.18
Area strain (%)	20.1 ± 17.6	41.0 ± 19.8	0.004
Mean segmental strains			
Radial strain (%)	-16.4 ± 6.2	-19.3 ± 8.4	0.26
Circumferential strain (%)	12.2 ± 8.9	17.7 ± 8.8	0.08
Longitudinal strain (%)	20.6 ± 10.7	34.4 ± 10.5	0.0005
3D strain (%)	-10.3 ± 4.9	-12.2 ± 5.8	0.30
Area strain (%)	28.1 ± 19.8	49.1 ± 19.7	0.004

Abbreviations: 3D = three-dimensional, cTOF = corrected tetralogy of Fallot

Three-dimensional speckle tracking echocardiography-derived peak strain parameters. Global and mean segmental peak longitudinal and area strain parameters and global peak radial strain proved to be reduced in cTOF patients as compared to controls (Table 7). Segmental peak strain parameters are summarized in Table 8.

Table 8. Comparison of three-dimensional speckle-tracking echocardiography-derived segmented peak right atrial strain parameters in patients with corrected tetralogy of Fallot and controls

	cTOF patients (n=17)	Controls (n=18)	p-value
RS_{basal} (%)	-16.1 ± 9.0	-17.3 ± 7.6	0.67
RS_{mid-atrial} (%)	-17.4 ± 7.5	-18.3 ± 10.7	0.78
RS_{superior} (%)	-15.2 ± 9.8	-23.6 ± 12.1	0.03
CS_{basal} (%)	10.9 ± 10.0	24.2 ± 11.4	0.0009
CS_{mid-atrial} (%)	11.0 ± 8.2	15.1 ± 8.9	0.17
CS_{superior} (%)	16.7 ± 14.5	11.0 ± 12.1	0.21
LS_{basal} (%)	19.8 ± 12.4	32.7 ± 12.3	0.004
LS_{mid-atrial} (%)	28.8 ± 16.1	49.6 ± 15.3	0.0004
LS_{superior} (%)	10.7 ± 7.7	14.2 ± 12.5	0.33
3DS_{basal} (%)	-10.2 ± 5.45	-10.6 ± 5.7	0.83
3DS_{mid-atrial} (%)	-10.7 ± 5.5	-10.2 ± 6.5	0.81
3DS_{superior} (%)	-10.0 ± 5.9	-17.7 ± 10.9	0.01
AS_{basal} (%)	21.9 ± 17.4	50.1 ± 18.0	<0.0001
AS_{mid-atrial} (%)	35.3 ± 25.7	64.3 ± 26.0	0.002
AS_{superior} (%)	28.9 ± 23.3	25.0 ± 26.1	0.64

Abbreviations: RS = radial strain, CS = circumferential strain, LS = longitudinal strain, 3DS = three-dimensional strain, AS = area strain, cTOF = corrected tetralogy of Fallot

Three-dimensional speckle tracking echocardiography-derived strain parameters at atrial contraction. Global circumferential and 3D strain parameters at atrial contraction were found to be reduced in cTOF patients as compared to controls (Table 9). Segmental strain parameters at atrial contraction are summarized in Table 10.

Table 9. Comparison of three-dimensional speckle-tracking echocardiography-derived global and segmental pre-atrial contraction right atrial strain parameters in patients with corrected tetralogy of Fallot and controls

	cTOF patients (n=17)	Controls (n=18)	p-value
Global strains			
Radial strain (%)	-5.7 ± 4.3	-8.0 ± 8.3	0.31
Circumferential strain (%)	3.9 ± 6.9	10.8 ± 11.0	0.03
Longitudinal strain (%)	5.7 ± 6.3	8.7 ± 9.6	0.29
3D strain (%)	-1.5 ± 4.2	-5.6 ± 5.4	0.02
Area strain (%)	10.0 ± 13.2	16.6 ± 17.0	0.21
Mean segmental strains			
Radial strain (%)	-7.3 ± 5.3	-9.0 ± 5.4	0.34
Circumferential strain (%)	7.4 ± 9.2	3.5 ± 9.8	0.24
Longitudinal strain (%)	7.3 ± 5.2	9.3 ± 6.4	0.33
3D strain (%)	-4.6 ± 4.7	-7.1 ± 4.8	0.13
Area strain (%)	13.5 ± 13.2	21.3 ± 15.6	0.12

Abbreviations: 3D = three-dimensional, cTOF = corrected tetralogy of Fallot

Table 10. Comparison of three-dimensional speckle-tracking echocardiography-derived segmental right atrial strain parameters at atrial contraction in patients with corrected tetralogy of Fallot and controls

	cTOF patients	Controls	p-value
	(n=17)	(n=18)	
RS_{basal} (%)	-7.3 ± 7.3	-9.6 ± 6.5	0.32
RS_{mid-atrial} (%)	-7.8 ± 5.2	-8.5 ± 6.0	0.69
RS_{superior} (%)	-6.5 ± 8.3	-8.9 ± 7.1	0.36
CS_{basal} (%)	5.3 ± 8.4	16.8 ± 9.8	0.0008
CS_{mid-atrial} (%)	5.7 ± 6.4	11.4 ± 8.8	0.04
CS_{superior} (%)	7.1 ± 9.6	9.7 ± 13.2	0.52
LS_{basal} (%)	7.1 ± 4.0	6.7 ± 5.7	0.83
LS_{mid-atrial} (%)	9.4 ± 8.8	9.7 ± 7.5	0.92
LS_{superior} (%)	5.6 ± 6.3	10.2 ± 9.6	0.11
3DS_{basal} (%)	-4.9 ± 5.8	-7.7 ± 5.7	0.17
3DS_{mid-atrial} (%)	-4.6 ± 4.6	-6.0 ± 4.6	0.37
3DS_{superior} (%)	-4.4 ± 8.5	-7.5 ± 6.0	0.21
AS_{basal} (%)	11.9 ± 12.7	19.9 ± 11.2	0.06
AS_{mid-atrial} (%)	16.0 ± 16.5	24.3 ± 14.8	0.13
AS_{superior} (%)	12.7 ± 16.4	18.7 ± 31.9	0.50

Abbreviations: RS = radial strain, CS = circumferential strain, LS = longitudinal strain, 3DS = three-dimensional strain, AS = area strain, cTOF = corrected tetralogy of Fallot

Reproducibility of volumetric three-dimensional speckle tracking echocardiographic measurements. The differences expressed as mean \pm standard deviation in values obtained by 2 measurements of the same observer for the measurements of 3DSTE-derived maximum and minimum LA volumes and LA volume before atrial contraction in cTOF patients were -2.0 ± 10.3 ml, -2.3 ± 11.3 ml, -3.0 ± 10.8 ml, respectively. Correlation coefficients between the 2 measurements of the same observer measurements of 2 observers were 0.99, 0.98 and 0.99 ($p < 0.0001$), respectively (Figures 3-5) (intraobserver agreement). The differences expressed as mean \pm standard deviation in values obtained by two observers for 3DSTE-derived maximum and minimum LA volumes and LA volume before atrial contraction in cTOF patients were 0.6 ± 10.0 ml, -1.5 ± 9.2 ml, -2.3 ± 20.4 ml, respectively. Correlation coefficient between these independent measurements of the two observers the same observer were 0.99, 0.99 and 0.95 ($p < 0.0001$), respectively (Figures 4-6) (interobserver agreement).

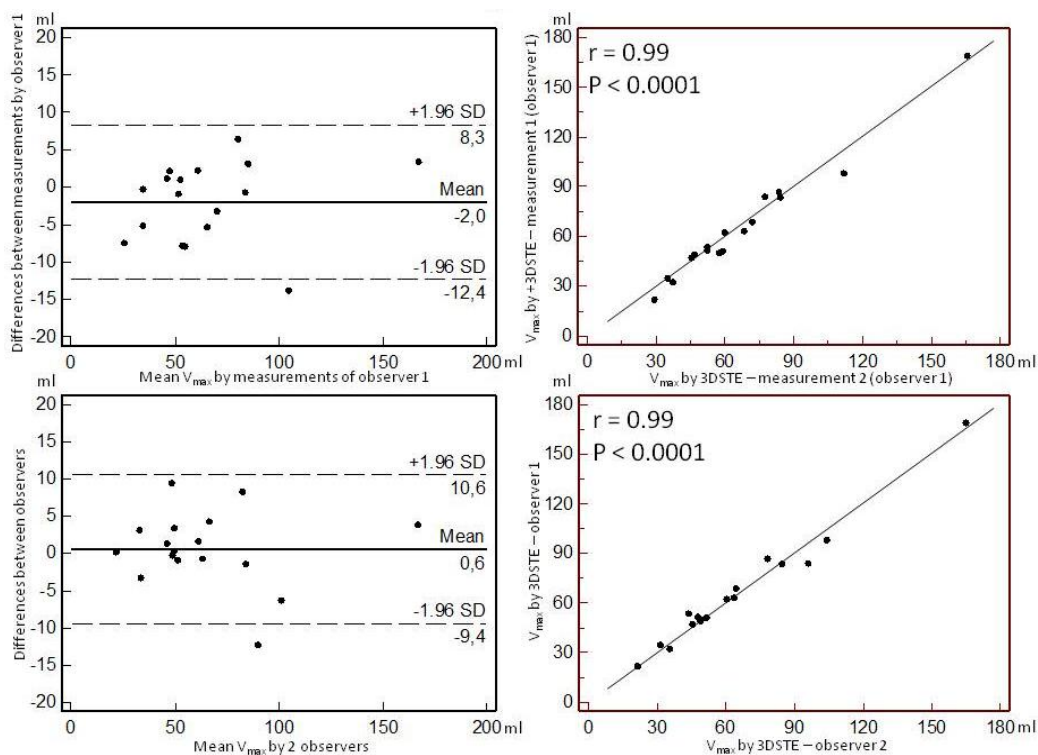


Figure 4. Intraobserver (upper graphs) and interobserver (lower graphs) agreements and correlations for measuring peak V_{\max} by three-dimensional speckle-tracking echocardiography are presented.

Abbreviations: V_{\max} = maximum right atrial volume, 3DSTE = three-dimensional speckle tracking echocardiography

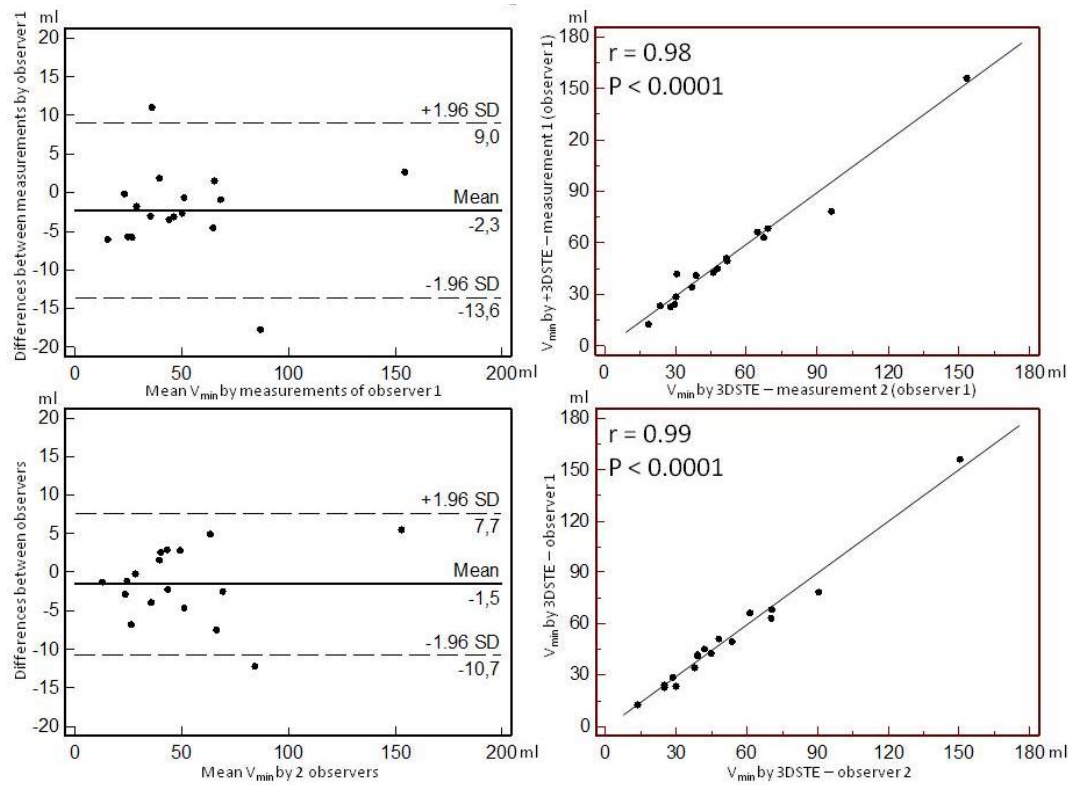


Figure 5 Intraobserver (upper graphs) and interobserver (lower graphs) agreements and correlations for measuring peak V_{\min} by three-dimensional speckle-tracking echocardiography are presented.

Abbreviations: V_{\min} = minimum right atrial volume, 3DSTE = three-dimensional speckle tracking echocardiography

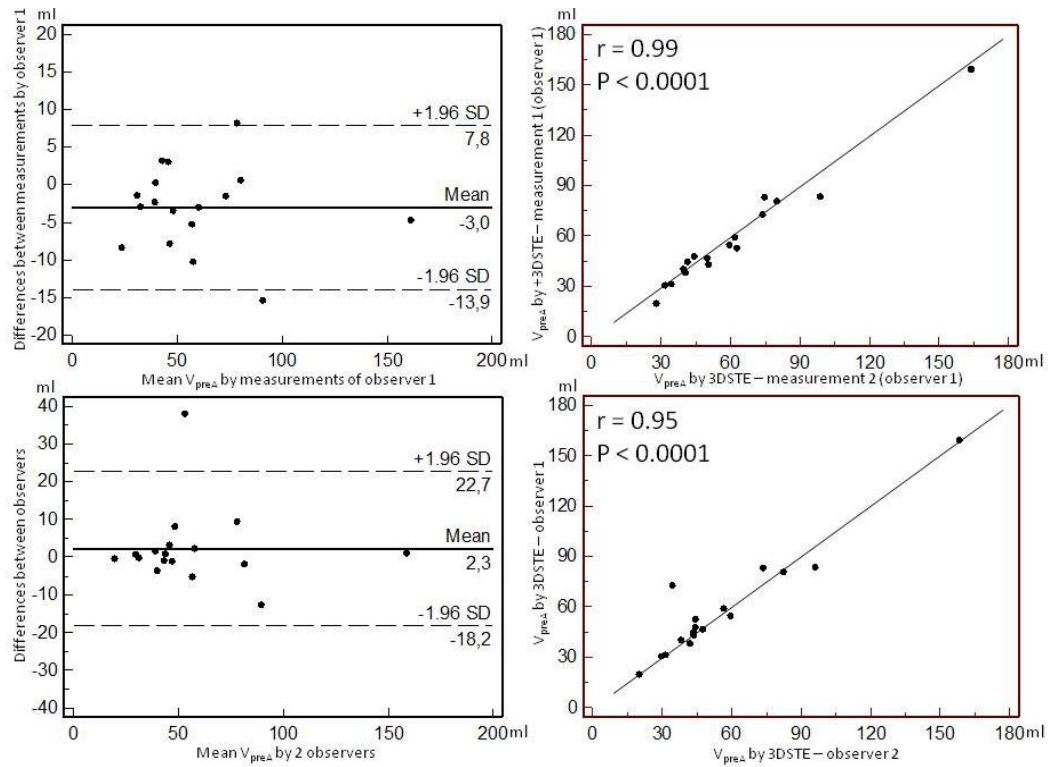


Figure 6 Intraobserver (upper graphs) and interobserver (lower graphs) agreements and correlations for measuring peak V_{preA} by three-dimensional speckle tracking echocardiography are presented.

Abbreviations: V_{preA} = right atrial volume before atrial contraction, 3DSTE = three-dimensional speckle tracking echocardiography

4.2.2. Left atrial deformation analysis in patients with corrected tetralogy of Fallot

Patient populations. Nineteen consecutive adult patients with cTOF in sinus rhythm were willing to participate in the present study (mean age: 37.9 ± 11.3 years, 8 men) who had repair at the age of 4.1 ± 2.5 years. In our department, several hundreds of healthy control subjects without risk factors or known disorders from different age groups were examined by 3DSTE to assess the normal values of 3DSTE-derived parameters. From this pool, 20 age- and gender matched healthy subjects (mean age: 39.2 ± 10.6 years, 14 men) were selected who served as a control group in this particular study.

Clinical data. Risk factors, medications applied and two-dimensional echocardiographic data are presented in Table 11. Significant ($>$ grade 2) mitral and tricuspid regurgitations could be detected in 2 (11%) and 8 (42%) cTOF patients. None of the healthy controls had significant regurgitations. The TAPSE and RV-FAC values of cTOF patients proved to be 18.2 ± 4.6 mm and $34.2 \pm 3.9\%$, respectively.

3DSTE-derived LA volumes and volume-based functional properties. Increased LA volumes and reduced LA emptying fractions respecting the cardiac cycle could be demonstrated in cTOF patients compared to controls. LA stroke volumes featuring all LA functions showed no differences between the groups examined (Table 12).

3DSTE-derived LA peak strain parameters. LA global and mean segmental uni- and multidirectional strains featuring LA reservoir function were found to be diminished in adult patients with cTOF as compared to controls (Table 13).

Table 11. Demographic and clinical data of patients with tetralogy of Fallot and that of controls

	ꞵTOF patients (n=19)	Controls (n=23)	p-value
Risk factors			
Age (years)	37.9 ± 11.3	39.2 ± 10.6	0.70
Male gender (%)	8 (42)	14 (61)	0.35
Hypertension (%)	3 (16)	0 (0)	0.08
Hypercholesterolemia (%)	1 (5)	0 (0)	0.45
Diabetes mellitus (%)	0 (0)	0 (0)	1.00
Medications			
β-blockers (%)	5 (26)	0 (0)	0.01
ACE-inhibitors (%)	3 (16)	0 (0)	0.08
Diuretics (%)	3 (16)	0 (0)	0.08
Two-dimensional echocardiography			
LA diameter (mm)	42.4 ± 6.8	33.2 ± 3.8	<0.0001
LV end-diastolic diameter (mm)	54.6 ± 19.6	48.3 ± 6.9	0.16
LV end-diastolic volume (ml)	113.7 ± 31.7	102.2 ± 21.1	0.17
LV end-systolic diameter (mm)	32.7 ± 7.1	30.4 ± 4.1	0.20
LV end-systolic volume (ml)	43.8 ± 23.2	35.6 ± 10.6	0.14
Interventricular septum (mm)	9.9 ± 1.5	9.5 ± 2.0	0.46
LV posterior wall (mm)	9.8 ± 1.5	9.4 ± 2.3	0.55
LV ejection fraction (%)	62.7 ± 11.5	65.4 ± 6.5	0.34

Abbreviations: ACE = angiotensin-converting enzyme, LA = left atrial, LV = left ventricular

Table 12. Comparison of 3DSTE-derived volumes and volume-based functional properties between patients with corrected tetralogy of Fallot and controls

	Calculated volumes (ml)			Stroke volumes (ml)			Emptying fractions (%)		
	V_{\max}	V_{\min}	V_{preA}	TASV	PASV	AASV	TAEF	PAEF	AAEF
cTOF patients	53.3 ± 28.1	35.1 ± 24.4	42.7 ± 26.0	18.2 ± 7.4	10.6 ± 6.4	7.6 ± 4.4	37.1 ± 11.7	21.4 ± 11.6	20.1 ± 10.8
Controls	36.8 ± 6.6	18.2 ± 6.3	26.3 ± 8.1	18.6 ± 4.1	10.5 ± 4.6	8.1 ± 3.2	51.4 ± 11.4	29.5 ± 13.3	31.1 ± 9.1
p value	0.009	0.003	0.006	0.84	0.96	0.71	0.0003	0.04	0.0009

Abbreviations: 3DSTE = three-dimensional speckle-tracking echocardiography, V_{\max} = maximum left atrial volume, V_{\min} = minimum left atrial volume, V_{preA} = left atrial volume at atrial contraction, TASV = total atrial stroke volume, TAEF = total atrial emptying fraction, PASV = passive atrial stroke volume, PAEF = passive atrial emptying fraction, AASV = active atrial stroke volume, AAEF = active atrial emptying fraction, cTOF = corrected tetralogy of Fallot

Table 13. Comparison of 3DSTE-derived peak strains and strains at atrial contraction between patients with tetralogy of Fallot and controls (global and mean segmental parameters).

	Radial strain (%)		Circumferential strain (%)		Longitudinal strain (%)		Three-dimensional strain (%)		Area strain (%)	
	Global	Mean segmental	Global	Mean segmental	Global	Mean segmental	Global	Mean segmental	Global	Mean segmental
Peak strains										
cTOF patients	-12.8 ± 9.5	-17.0 ± 8.5	13.2 ± 9.2	18.3 ± 8.8	17.4 ± 8.3	19.7 ± 8.1	-7.0 ± 6.3	-11.5 ± 6.2	33.1 ± 14.2	38.9 ± 13.7
Controls	-18.0 ± 9.9	-21.7 ± 8.9	29.0 ± 13.4	34.2 ± 13.1	26.3 ± 7.7	29.6 ± 7.4	-11.0 ± 8.2	-15.1 ± 6.9	59.7 ± 22.0	67.9 ± 21.7
p value	0.10	0.09	0.0001	0.0001	0.0008	0.0002	0.09	0.09	0.0001	<0.0001
Strains at atrial contraction										
cTOF patients	-2.8 ± 4.6	-6.5 ± 5.6	4.5 ± 5.0	7.3 ± 5.0	2.9 ± 4.6	4.7 ± 3.9	-1.7 ± 6.4	-4.7 ± 4.8	8.1 ± 9.7	12.4 ± 8.9
Controls	-7.2 ± 7.9	-8.2 ± 5.5	11.2 ± 10.4	13.9 ± 9.2	8.1 ± 8.8	9.0 ± 5.8	-5.5 ± 5.1	-6.4 ± 4.8	16.7 ± 16.1	20.3 ± 14.2
p value	0.03	0.33	0.01	0.008	0.03	0.10	0.04	0.24	0.04	0.04

Abbreviations: 3DSTE = three-dimensional speckle-tracking echocardiography, cTOF = corrected tetralogy of Fallot

3DSTE-derived LA strain parameters at atrial contraction. Similarly to peak strains, reduced global and mean segmental LA strains at atrial contraction characterizing atrial booster pump function could be demonstrated in cTOF patients as compared to controls (Table 13).

4.3. Detection of left ventricular 'rigid body rotation' in certain congenital heart diseases

4.3.1. "Rigid body rotation" of the left ventricle in hypoplastic right heart syndrome

A 19-year-old girl with surgically palliated hypoplastic right heart syndrome (HRHS) with intact ventricular septum, ostium secundum ASD and small RV cavity is presented. The patient had undergone palliation with a superior vena cava to pulmonary artery shunt (bidirectional Glenn) at 3 years of age. A complete 2D Doppler echocardiography was carried out extended with a 3DSTE (Figure 9). The movement of the septum was found to be dyskinetic.

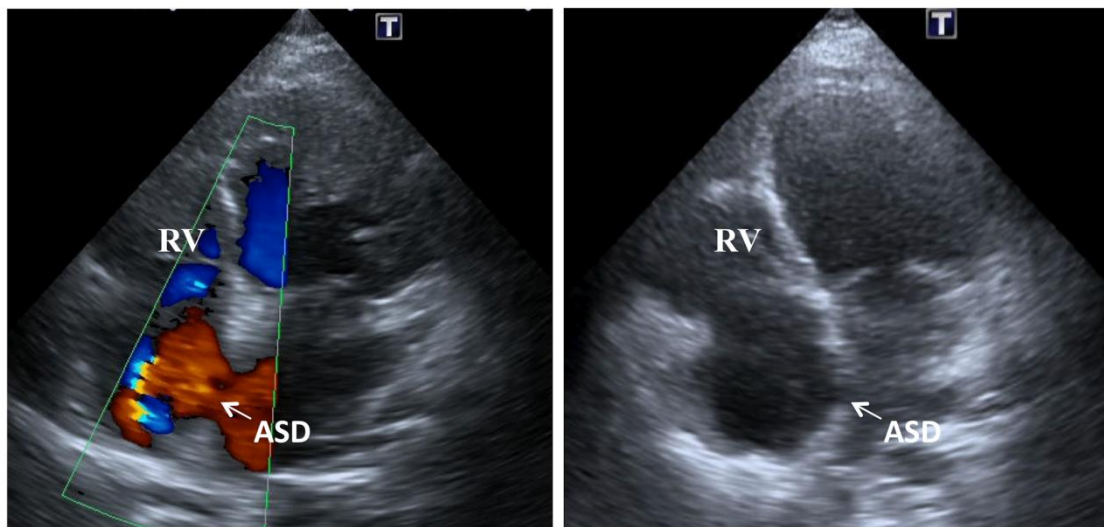


Figure 9. Transthoracic Doppler echocardiography images from a 19-year-old girl with palliated hypoplastic right heart syndrome. The images demonstrate an intact ventricular septum, atrial septal defect (ASD), and small right ventricular (RV) cavity.

The multiple long- (A, B) and short-axis views (C3, C5, C7) extracted from 3D echocardiographic datasets of the patient with HRHS and that of a healthy control are demonstrated in Figures 10 and 11. Visual information on LV rotational mechanics is shown in colour overlay superimposed on grey-scale images in both cases.

LV end-diastolic and end-systolic volumes, ejection fraction, mass and RV outflow tract and tricuspid annular plane systolic excursion of the patient proved to be 107 ml, 64 ml, 40%, 198 g, 17 mm and 14 mm, respectively. Results of the present case with HRHS suggest that all LV regions move in almost the same clockwise direction (Figure 10F, dashed arrow, negative value).

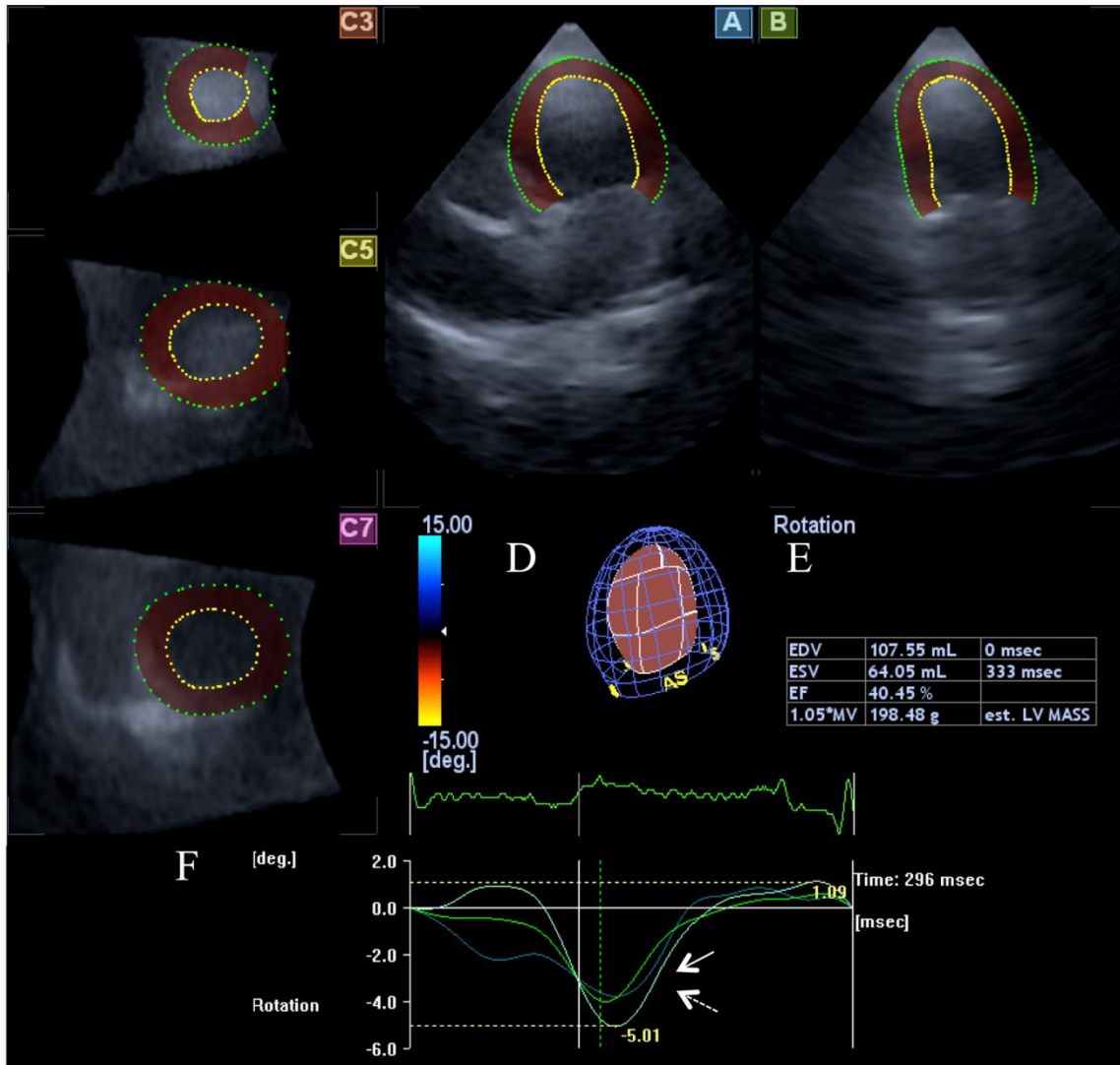


Figure 10. In a patient with palliated hypoplastic right heart syndrome, apical 4-chamber (A) and 2-chamber (B) views and short-axis views (C3, C5, C7) at different levels of the left ventricle extracted from the three-dimensional echocardiographic dataset are presented. A three-dimensional cast of the left ventricle (D) and calculated volumetric and functional left ventricular parameters (EDV = end-diastolic volume, ESV = end-systolic volume, EF = ejection fraction) are also demonstrated (E). Left ventricular basal and apical rotations proved to be in the same clockwise direction with near absence of left ventricular twist (F).

Global LV RS, CS, LS, 3DS and AS parameters and the range for all segments proved to be $5.1 \pm 4.3\%$, $-12.2 \pm 8.0\%$, $-14.1 \pm 8.5\%$, $6.0 \pm 4.8\%$, $-24.3 \pm 13.8\%$, respectively.

Quantitative data of LV rotation of the control subject demonstrates adequate rotational directions with counterclockwise motion of the LV apex (white arrow, positive value) and clockwise motion of the LV base (dashed arrow, negative value) (Figure 11F).

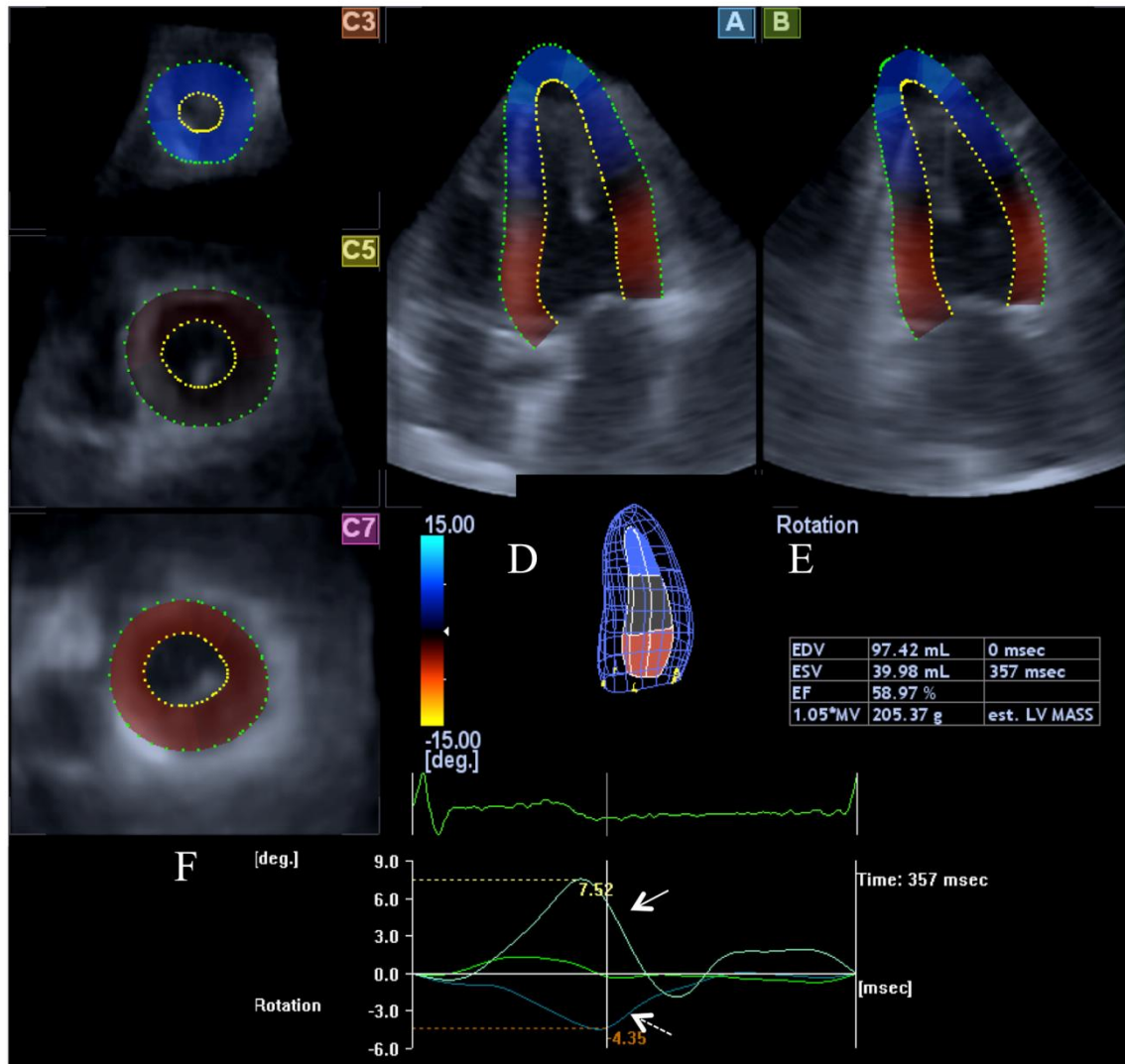


Figure 11. In a healthy subject, apical 4-chamber (A) and 2-chamber (B) views and short-axis views (C3, C5, C7) at different levels of the left ventricle extracted from the three-dimensional echocardiographic dataset are presented. A three-dimensional cast of the left ventricle (D) and calculated volumetric and functional left ventricular parameters (EDV = end-diastolic volume, ESV = end-systolic volume, EF = ejection fraction) are also demonstrated (E). Counterclockwise rotation of the left ventricular apex (white arrow, positive value) and clockwise rotation of the left ventricular base (dashed arrow, negative value) are shown demonstrating normal rotational directions (F).

4.3.2. Left ventricular 'rigid body rotation' in a patient with an univentricular heart

A 18 year-old boy with an univentricular heart due to tricuspid atresia after Fontan procedure with LV characteristics is presented, who was examined with standard 2D echocardiography and 3DSTE at the Cardiology Center of University of Szeged, Hungary. 2D echocardiography confirmed univentricular heart (Figure 12).

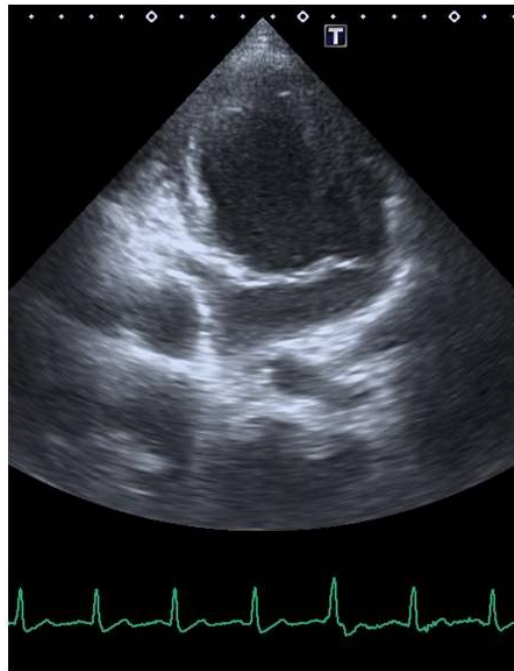


Figure 12. An 18 year-old boy with univentricular heart is presented by transthoracic echocardiography

Three short-axis views and AP4CH and AP2CH views extracted from 3D echocardiographic datasets are demonstrated in Figure 13. During 3DSTE analysis, severely decreased basal and apical rotations which were in the same counterclockwise direction with near absence of twist called as "rigid body rotation" of the LV could be detected.

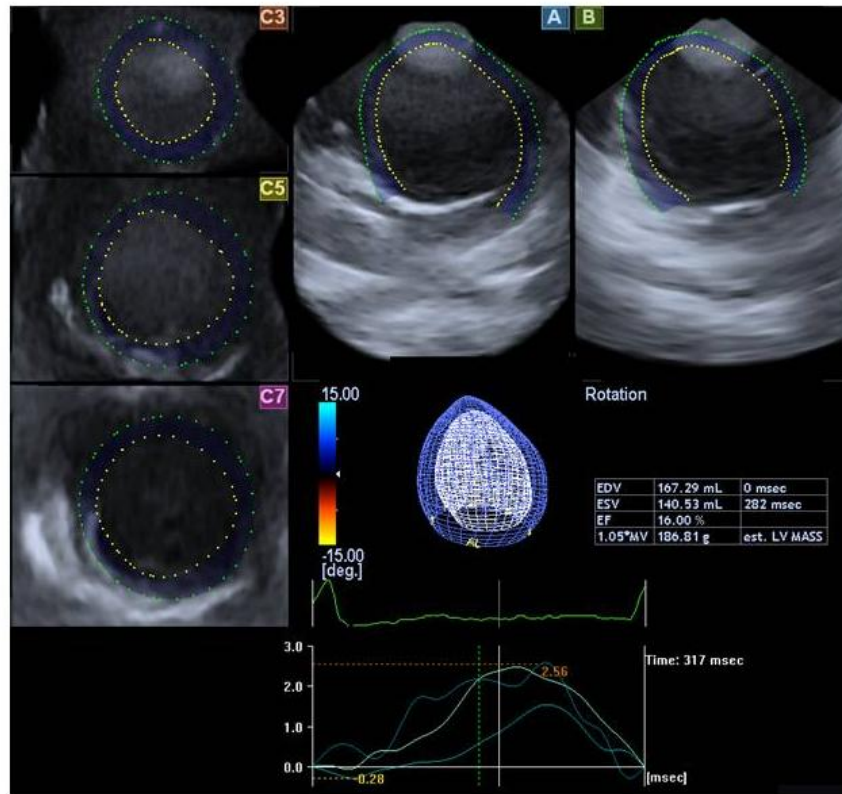


Figure 13. Apical 4-chamber (A) and 2-chamber (B) views and short-axis views (C3, C5, C7) at different levels of the left ventricle (LV) extracted from the three-dimensional (3D) echocardiographic dataset are presented. A 3D cast of the LV and calculated volumetric and functional LV parameters (EDV: end-diastolic volume, ESV: end-systolic volume, EF: ejection fraction, estimated LV mass) are also demonstrated. LV basal and apical rotations proved to be in the same counterclockwise direction with near absence of LV twist in the patient with univentricular heart (F).

5. Discussion

5.1. Long-term follow-up of patients with transposition of the great arteries following Senning or Mustard operations

Expected survival of TGA increases due to development of surgical techniques, therefore the number of these patients gradually increases in the adult cardiology patient care. Therefore it is important for colleagues working in patient care to know the basics of the disease, past and present surgical solutions and possible clinical problems (residual vitium, heart failure, arrhythmias, baffle-related complications, etc.). The primary treatment of TGA is to keep communication between the two circulations in early infancy (7). Accordingly, firstly palliative surgery is performed, and later following weight gain of the child it is aimed to eliminate the shunt via a reconstructive procedure (7). Initially, only the Blalock-Hanlon surgery could be performed as a palliative procedure, when atrial communication is established between the two circulations by the excision of the atrial septum. Later, with technical development, Rashkind balloon septostomy became widely used, during this procedure, the atrial septum is fenestrated by a catheter balloon (30). Senning and Mustard reconstructive (switch) surgeries performed at atrial level were the most widely used procedures in the second part of the last century (7). Senning and Mustard operations are similar procedures, they differ only in the technique of creating the baffle. While during a Senning procedure, more own tissue was used to form a baffle between the atria, during Mustard technique, the blood was shepherd to the haemodinamically (not anatomically) correct atrio-ventricular valve via a pant-like patch made of foreign material. It is important to know, that if ventricular septal defect and stenosis of the pulmonary valve were also associated with TGA, Rastelli surgery was also an available option (31). In this case, the two circulations were divided by directing the blood from the LV through the ventricular defect to the aorta originating from the RV by closing the ventricular septal defect, so that a spot remains between the RV body and the infundibulum. The remaining RV body is connected to the pulmonary artery with an extracardiac conduit. From the 1990s, the above procedures have been replaced by the neonatal arterial switch surgery, when the two great arteries (aorta and pulmonary artery) are transected and interchanged, then the pulmonary arteries are sutured to the RV and the aorta to the LV, and the coronary arteries are replaced to the pulmonary artery supplying the systemic circulation (32).

In elaboration of the above detailed reconstructive operations, several -Hungarian heart surgeon colleagues have pioneered. Heart surgeries due to congenital heart diseases have been performed since 1962 at the Independent Department of Heart Surgery, University of Szeged, later at the Cardiology Center. At the beginning, only palliative surgeries could be performed, the first Rashkind septostomy was performed in Szeged in 1967 (33). Both reconstructive surgeries performed at atrial level were applied only in Szeged in Hungary. The first Mustard operation was performed in 1969 by Prof. Gábor Kovács, later this technique together with its modified Brom version were applied until 1985 all together in 48 cases. In that year, two operations were performed (one Mustard and one Senning operation). The Senning technique, when baffle was not used in some cases, only the remaining septum was sutured to the influx of the pulmonary veins, was applied in 37 cases.

The present study aimed to compare long-term results of two similar, but technically different surgical procedures with respect to survival, different clinical characteristics (baffle-related complications, heart failure, arrhythmologic complications) and quality of life. It could be said that mortality and morbidity data of Senning and Mustard surgery populations did not differ significantly. Although comparing quality of life data showed that the results of Senning operated patients were more favourable. However, it could be explained by the lower age and shorter follow-up period. These facts are important, because these two methods were the only possible approaches to treat TGA in the past. Although arterial switch operation (called as Jatene surgery) is the applicable procedure nowadays, there is a significant population with a history of surgery performed at atrial level who turn to adult cardiologists due to the favourable survival of these surgeries. TGA is a relatively rare congenital heart disease, and there are no analytical evidences based on results of many patients. Therefore, we tried to collect patient data and draw conclusions from our patients helping the success of long-term treatment in this study.

In a recent Hungarian follow-up work it was found, that certain laboratory (B-natriuretic peptide), echocardiographic (Tei-index), and some magnetic resonance imaging parameters were suitable to screen and assess RV function of TGA patients after Senning operation. It was highlighted that two-stage anatomical correction of the TGA is required to protect the LV at younger ages, even without symptoms (34). In a national Belgian work, a similar study was performed summarizing results of six centers with similar patient numbers per center (35). The two surgical techniques were applied at the same time in this study as opposed to the study performed in our University where only Mustard operation was

performed first, then only Senning operation was performed. Similarly to our results, mortality of the two methods did not differ, but Senning operated patients were in favourable functional condition, they had more pronounced sport activity and less baffle-related complications (35). In another Danish-Swedish study, long-term follow-up of the two surgical techniques was examined (36). It was found that long-term survival shows a higher correlation with RV and tricuspid valve function, than with the type of surgery and its date. It was also confirmed that necessity of pacemaker implantation was related to mortality in these patients. In addition to the above mentioned results, several other studies have examined long-term efficiency of Mustard and Senning surgeries (5, 37-40).

Important limitations. The most important limitation is the relatively low number of patients and the 74% follow-up ratio. However, in view of national conditions and the actuality of the problem, and despite the above mentioned limitations, it was found to be important to publish our results. Moreover, the two compared surgical techniques were not performed in parallel, but in two consecutive periods. Therefore, the duration of the follow-up and the age of patients were different, which could theoretically affect our results. Although NT-proBNP measurement was performed in some cases and echocardiographic examination was performed in all subjects, it was not possible to compare them between the groups due to incomplete data and parameters (non-conventional medical records).

5.2. Volumetric and functional evaluation of atria in corrected tetralogy of Fallot

5.2.1. Detailed evaluation of right atrial dysfunction in patients with corrected tetralogy of Fallot

To the best of the authors' knowledge, this is the first study in which RA volumetric and functional changes could be demonstrated in patients with cTOF by 3DSTE. Results confirm previous findings, that 3DSTE enables more detailed evaluation of atrial function respecting its motion during the cardiac cycle. Increased RA volumes and decreased RA emptying fractions were found together with alterations in global, mean segmental and segmental peak RA strains and strains at atrial contraction in cTOF patients.

Nowadays computed tomography, cardiac magnetic resonance imaging, transthoracic and transoesophageal volumetric real-time 3D echocardiography could be used in clinical

practice to provide reliable information on RA structures and function (41). Normative values for RA volumes and function were demonstrated by volumetric real-time 3D echocardiography and 2DSTE in a relatively large cohort of healthy subjects with a wide age range (42). 3DSTE is a novel cardiac imaging technique to assess complex cardiac motion based on frame-to-frame tracking of ultrasonic speckles in 3D (25, 26, 43). This methodology has been confirmed to be a promising tool for quantification of LV (44-46) and LA (27, 28, 47) volumes. Moreover, global and regional LV (48-50), RV (10) and LA (28, 29, 51) myocardial deformation could also be assessed by 3D strain analysis. There is an opportunity of measuring dyssynchrony of parameters by 3DSTE, as demonstrated that of LV (52-54), LA (51) and RV (10), as well. However, volumetric and functional evaluations of RA have never been assessed by 3DSTE.

In recent studies, alterations in ventricular deformations could be demonstrated in adult cTOF patients by 3DSTE (10, 11, 53). Impaired global and regional LV 3D systolic strain, mechanical dyssynchrony, and reduced twist were found to be related to reduced septal curvature in repaired tetralogy of Fallot patients with and without pulmonary valve replacement (53). In another study performed with adults after tetralogy of Fallot repair, 3D RV deformation was found to be impaired in association with RV dyssynchrony, volume overloading, and reduced ejection fraction (10). However, atrial deformation has never been assessed by 3DSTE in cTOF.

During evaluation of RA, all three functions have been assessed including [1] reservoir function by total atrial stroke volume (TASV) and total atrial emptying fraction (TAEF) together with global, mean segmental and segmental basal, mid-atrial and superior peak strain parameters, [2] conduit function by passive atrial stroke volume (PASV) and passive atrial emptying fraction (PAEF), and [3] active contraction by active atrial stroke volume (AASV) and active atrial emptying fraction (AAEF) together with global, mean segmental and segmental basal, mid-atrial and superior strain parameters at atrial contraction. Regarding to our volumetric measurements, reduced reservoir (decreased TAEF) and conduit (reduced PAEF) functions could be demonstrated. Alterations in specific global, mean segmental and segmental RA peak strains confirmed diminished RA reservoir function. While AASV and AAEF showed no significant alterations, global and specific segmental RA strains at atrial contraction showed reduction suggesting changes in active contraction phase, as well. Reduced RA function could be explained by hydrodynamic effects of pulmonary and/or

tricuspid regurgitation, scar in the RA, injured pericardium, and the disease itself (55). However, further studies are warranted to confirm our findings.

Limitation section. The following important limitations should be taken into consideration when interpreting our results:

- (1) RA appendage, caval veins and sinus coronarius were excluded from the calculation of RA volumes and functional properties.
- (2) Current image quality obtained by 3DSTE is worse than that of 2D echocardiography due to low temporal and spatial image resolutions.
- (3) 3DSTE was used for calculation of volumetric (27, 28, 46) and strain (28, 29, 51) parameters of the RA validated for LA (27-29, 46, 51). However, further validation studies are warranted by other imaging tools for both atria.
- (4) Reproducibility assessments were calculated only for peak volumetric RA data due to the fact, that volumetric and strain assessments were performed from the same 3D echocardiographic datasets.
- (5) RA dilation could have resulted from tricuspid regurgitation, which could also affect RA function.
- (6) LV, LA and RV deformations were not assessed by 3DSTE in this study.
- (7) We did not aim to find relationship between morphology and function of the RV and RA.
- (8) This was a single-center experience and limited by a relatively small number of cTOF patients. The study would have been statistically stronger, if larger number of subjects had been evaluated.

5.2.2. Left atrial deformation analysis in patients with corrected tetralogy of Fallot

The study reported here is the first to analyse 3DSTE-derived LA deformation in adult patients with cTOF. Increased LA volumes and diminished LA emptying fractions and strains could be demonstrated in this detailed analysis. Results suggest significant deterioration of all LA functions (reservoir, conduit and booster pump) in adult patients with cTOF late after repair.

STE was found to be a valuable tool for volumetric and functional assessment of cardiac chambers in adult patients with cTOF (10, 11, 56). In a recent study, RV free wall strain and strain rate were found to be decreased in adults late after TOF repair, especially at the apical segment suggesting that apical function is the most affected in these RVs (11). Regarding the LV, septal strain was decreased indicating that RV dysfunction adversely affects LV function, probably by mechanical coupling of the ventricles. In another study, the majority of adults with cTOF showed reduced LV twist (57). Strikingly, one-quarter of these patients had an abnormal apical rotation which was found to be associated with decreased systolic LV and RV function. These findings suggested that abnormal apical rotation could be a new objective diagnostic criterion for detection of ventricular dysfunction in cTOF.

The complexity of RA dysfunction could also be demonstrated by 3DSTE in cTOF patients (56). Comparing this with the present study, both RA and LA volumes seemed to be increased in adult patients with cTOF. Moreover, large similarity of RA and LA deformation could also be demonstrated: while RA/LA emptying fractions were found to be decreased, RA/LA stroke volumes remained unchanged. All peak LA strains and LA strains at atrial contraction were found to be reduced and this reduction was more pronounced in cTOF as compared to the values related to RA. Therefore examination of LA seems to be important in the follow-up of cTOF patients. Other studies have also found that LA plays an important part in the development of late complications in cTOF patients (58). Several factors may play a role in the altered atrial function in cTOF, such as the interaction between both atria, the presence of mitral/tricuspid regurgitation, arrhythmias and changes in both ventricular features as demonstrated before. Further studies are warranted to understand the real pathophysiologic background of these findings.

Limitation section. Beyond the above mentioned limitations it should also be considered that during creation of the 3D model of the LA, the septum was considered to be part of the LA similarly to the previous study evaluating RA (56). Finally, LA appendage and pulmonary veins were excluded, which could theoretically affect the results.

5.3. Detection of left ventricular 'rigid body rotation' in special congenital diseases (hypoplastic right heart syndrome and univentricular heart)

To the best of the authors' knowledge, this is the first time to demonstrate that LV basal and apical rotations could be in the same clockwise direction with near absence of LV twist called as "rigid body rotation" of the LV in HRHS. Moreover, it is also the first time that a counterclockwise LV-RBR was found in a patient with univentricular heart.

Van Dalen *et al.* were the first to demonstrate LV-RBR in patients with noncompaction of the LV (16, 17). The near absence of LV twist was found to be an objective, quantitative, and reproducible functional criterion with good predictive value for the diagnosis of LV noncompaction (17). LV-RBR could be demonstrated in 53.3% of 60 NCCM patients (59). In another smaller study, 9 out of 9 NCCM patients showed LV-RBR (60). Other authors found sensitivity and specificity of LV-RBR for differentiating NCCM from non-specific "hypertrabeculation" of the LV to be 88% and 78%, respectively (17).

HRHS and univentricular heart are rare congenital heart defects where the heart, or its ventricles fail to develop appropriately. Although dramatic decrease in apical rotation could be demonstrated in patients with single ventricle using STE (velocity vector imaging) in a recent study (61), LV-RBR has never been found by STE in these diseases.

It is known that 2DSTE based on frame-by-frame tracking of speckle patterns created by interference of the ultrasound beam within the myocardial tissue in one plane is likely to be affected by geometric assumptions and the use of foreshortened apical views (9, 16, 17). 3SDTE detects speckles in the 3D space and, therefore, is able to merge benefits of 3D and STE allowing clinicians to visualize the heart as it is: a 3D organ (9). It was found to be a quantitative way to assess LV rotation and twist deformations (9, 60, 62).

In conclusion, LV-RBR was identified in a single patient with HRHS. This finding could be partially explained by the impairment of ventricle-to-ventricle interaction. The anatomic myocardial fiber orientation, which is a left-handed helix in the epicardium and a right-handed helix in the endocardium in normal situation, could be altered in this disease. This could also theoretically explain LV-RBR of our univentricular patient. However, other reasons could not be excluded, as well. Further studies with larger number of patients with congenital heart diseases are warranted to confirm our findings with deeper insights into pathophysiology.

6. Conclusions (new observations)

There are no significant differences in mortality and morbidity of patients with transposition of the great arteries after Senning and Mustard operations. Quality of life and functional capacity of patients after Senning operation are more favourable.

The complexity of right atrial dysfunction can be demonstrated by three-dimensional speckle-tracking echocardiography in patients with corrected tetralogy of Fallot.

Significant deterioration of all left atrial functions could be demonstrated in adult patients with corrected tetralogy of Fallot late after repair.

The near absence of left ventricular twist called as left ventricular 'rigid body rotation' could be demonstrated in selected congenital heart diseases like in patients with univentricular heart and hypoplastic right heart syndrome.

7. References

1. Baumgartner H, Bonhoeffer P, De Groot NM, de Haan F, Deanfield JE, Galie N, et al. ESC Guidelines for the management of grown-up congenital heart disease (new version 2010). *Eur Heart J*. 2010;31(23):2915-57.
2. Engelfriet P, Boersma E, Oechslin E, Tijssen J, Gatzoulis MA, Thilen U, et al. The spectrum of adult congenital heart disease in Europe: morbidity and mortality in a 5 year follow-up period. The Euro Heart Survey on adult congenital heart disease. *Eur Heart J*. 2005;26(21):2325-33.
3. In: Gatzoulis M, Webb, GD, Daubeney, PE, editor. Diagnosis and management of adult congenital heart disease. Edinburgh 2011.
4. Warnes CA. Transposition of the great arteries. *Circulation*. 2006;114(24):2699-709.
5. Ebenroth ES, Hurwitz RA. Functional outcome of patients operated for d-transposition of the great arteries with the Mustard procedure. *Am J Cardiol*. 2002;89(3):353-6.
6. Hartyanszky I, Varga S, Havasi K, Babik B, Katona M, Bogats G. [Perspectives in the management of congenital heart defects in adult patients]. *Orv Hetil*. 2015;156(3):92-7.
7. Konstantinov IE, Alexi-Meskishvili VV, Williams WG, Freedom RM, Van Praagh R. Atrial switch operation: past, present, and future. *Ann Thorac Surg*. 2004;77(6):2250-8.
8. Abduch MC, Alencar AM, Mathias W, Jr., Vieira ML. Cardiac mechanics evaluated by speckle tracking echocardiography. *Arq Bras Cardiol*. 2014;102(4):403-12.
9. Nemes A, Kalapos A, Domsik P, Forster T. [Three-dimensional speckle-tracking echocardiography -- a further step in non-invasive three-dimensional cardiac imaging]. *Orv Hetil*. 2012;153(40):1570-7.
10. Yu HK, Li SJ, Ip JJ, Lam WW, Wong SJ, Cheung YF. Right ventricular mechanics in adults after surgical repair of tetralogy of fallot: insights from three-dimensional speckle-tracking echocardiography. *J Am Soc Echocardiogr*. 2014;27(4):423-9.
11. Menting ME, van den Bosch AE, McGhie JS, Eindhoven JA, Cuypers JA, Witsenburg M, et al. Assessment of ventricular function in adults with repaired Tetralogy of Fallot using myocardial deformation imaging. *Eur Heart J Cardiovasc Imaging*. 2015;16(12):1347-57.
12. Nemes A, Havasi K, Domsik P, Kalapos A, Forster T. Evaluation of right atrial dysfunction in patients with corrected tetralogy of Fallot using 3D speckle-tracking echocardiography. Insights from the CSONGRAD Registry and MAGYAR-Path Study. *Herz*. 2015;40(7):980-8.

13. Nemes A, Kalapos A, Domsik P, Forster T. [Left ventricular rotation and twist of the heart. Clarification of some concepts]. *Orv Hetil.* 2012;153(39):1547-51.
14. Urbano Moral JA, Arias Godinez JA, Maron MS, Malik R, Eagan JE, Patel AR, et al. Left ventricular twist mechanics in hypertrophic cardiomyopathy assessed by three-dimensional speckle tracking echocardiography. *Am J Cardiol.* 2011;108(12):1788-95.
15. Sengupta PP, Tajik AJ, Chandrasekaran K, Khandheria BK. Twist mechanics of the left ventricle: principles and application. *JACC Cardiovasc Imaging.* 2008;1(3):366-76.
16. van Dalen BM, Caliskan K, Soliman OI, Nemes A, Vletter WB, Ten Cate FJ, et al. Left ventricular solid body rotation in non-compaction cardiomyopathy: a potential new objective and quantitative functional diagnostic criterion? *Eur J Heart Fail.* 2008;10(11):1088-93.
17. van Dalen BM, Caliskan K, Soliman OI, Kauer F, van der Zwaan HB, Vletter WB, et al. Diagnostic value of rigid body rotation in noncompaction cardiomyopathy. *J Am Soc Echocardiogr.* 2011;24(5):548-55.
18. Nemes A, Foldeak D, Domsik P, Kalapos A, Sepp R, Borbenyi Z, et al. Different patterns of left ventricular rotational mechanics in cardiac amyloidosis-results from the three-dimensional speckle-tracking echocardiographic MAGYAR-Path Study. *Quant Imaging Med Surg.* 2015;5(6):853-7.
19. The Criteria Committee of the New York Heart Association. Nomenclature and Criteria of the Diagnosis of Diseases of the Heart and Great Vessels. Boston: Little, Brown & Co; 1994.
20. Badia X, Monserrat S, Roset M, Herdman M. Feasibility, validity and test-retest reliability of scaling methods for health states: the visual analogue scale and the time trade-off. *Qual Life Res.* 1999;8(4):303-10.
21. Hinz A, Kohlmann T, Stobel-Richter Y, Zenger M, Brahler E. The quality of life questionnaire EQ-5D-5L: psychometric properties and normative values for the general German population. *Qual Life Res.* 2014;23(2):443-7.
22. Baecke JA, Burema J, Frijters JE. A short questionnaire for the measurement of habitual physical activity in epidemiological studies. *Am J Clin Nutr.* 1982;36(5):936-42.
23. Nemes A, Forster T. [Recent echocardiographic examination of the left ventricle - from M-mode to 3D speckle-tracking imaging]. *Orv Hetil.* 2015;156(43):1723-40.
24. Nemes A, Forster T. Echocardiographic assessment of the right ventricular morphology and function - From M-mode to 3D speckle -tracking. *Cardiol Hung.* 2016;46:171-83.

25. Urbano-Moral JA, Patel AR, Maron MS, Arias-Godinez JA, Pandian NG. Three-dimensional speckle-tracking echocardiography: methodological aspects and clinical potential. *Echocardiography*. 2012;29(8):997-1010.
26. Ammar KA, Paterick TE, Khandheria BK, Jan MF, Kramer C, Umland MM, et al. Myocardial mechanics: understanding and applying three-dimensional speckle tracking echocardiography in clinical practice. *Echocardiography*. 2012;29(7):861-72.
27. Nemes A, Domsik P, Kalapos A, Lengyel C, Orosz A, Forster T. Comparison of three-dimensional speckle tracking echocardiography and two-dimensional echocardiography for evaluation of left atrial size and function in healthy volunteers (results from the MAGYAR-Healthy study). *Echocardiography*. 2014;31(7):865-71.
28. Domsik P, Kalapos A, Chadaide S, Sepp R, Hausinger P, Forster T, et al. Three-dimensional speckle tracking echocardiography allows detailed evaluation of left atrial function in hypertrophic cardiomyopathy--insights from the MAGYAR-Path Study. *Echocardiography*. 2014;31(10):1245-52.
29. Chadaide S, Domsik P, Kalapos A, Saghy L, Forster T, Nemes A. Three-dimensional speckle tracking echocardiography-derived left atrial strain parameters are reduced in patients with atrial fibrillation (results from the MAGYAR-path study). *Echocardiography*. 2013;30(9):1078-83.
30. Cinteza E, Carminati M. Balloon atrial septostomy - almost half a century after. *Maedica (Buchar)*. 2013;8(3):280-4.
31. Squarcia U, Macchi C. Transposition of the great arteries. *Curr Opin Pediatr*. 2011;23(5):518-22.
32. De Praetere H, Vandesande J, Rega F, Daenen W, Marc G, Eyskens B, et al. 20 years of arterial switch operation for simple TGA. *Acta Chir Belg*. 2014;114(2):92-8.
33. Kovács G. History of heart surgery in Szeged. In: Kerkovits G, editor. 50 years history of the Hungarian Society of Cardiologists. Budapest: Convention Budapest Kft. ; 2007.
34. Hartyanszky I, Kadar K, Oprea V, Lozsadi K, Szabolcs J, Szatmari A. [Is the right ventricle able to maintain the systemic circulation for a long time? The late results of the Senning operation for complete transposition of the great arteries]. *Orv Hetil*. 2006;147(45):2155-60.
35. Moons P, Gewillig M, Sluysmans T, Verhaaren H, Viart P, Massin M, et al. Long term outcome up to 30 years after the Mustard or Senning operation: a nationwide multicentre study in Belgium. *Heart*. 2004;90(3):307-13.

36. Vejlstrup N, Sorensen K, Mattsson E, Thilen U, Kvidal P, Johansson B, et al. Long-Term Outcome of Mustard/Senning Correction for Transposition of the Great Arteries in Sweden and Denmark. *Circulation*. 2015;132(8):633-8.
37. Sarkar D, Bull C, Yates R, Wright D, Cullen S, Gewillig M, et al. Comparison of long-term outcomes of atrial repair of simple transposition with implications for a late arterial switch strategy. *Circulation*. 1999;100(19 Suppl):II176-81.
38. Poirier NC, Yu JH, Brizard CP, Mee RB. Long-term results of left ventricular reconditioning and anatomic correction for systemic right ventricular dysfunction after atrial switch procedures. *J Thorac Cardiovasc Surg*. 2004;127(4):975-81.
39. Meijboom F, Szatmari A, Deckers JW, Utens EM, Roelandt JR, Bos E, et al. Long-term follow-up (10 to 17 years) after Mustard repair for transposition of the great arteries. *J Thorac Cardiovasc Surg*. 1996;111(6):1158-68.
40. Moons P, De Bleser L, Budts W, Sluysmans T, De Wolf D, Massin M, et al. Health status, functional abilities, and quality of life after the Mustard or Senning operation. *Ann Thorac Surg*. 2004;77(4):1359-65; discussion 65.
41. Faletra FF, Muzzarelli S, Dequarti MC, Murzilli R, Bellu R, Ho SY. Imaging-based right-atrial anatomy by computed tomography, magnetic resonance imaging, and three-dimensional transoesophageal echocardiography: correlations with anatomic specimens. *Eur Heart J Cardiovasc Imaging*. 2013;14(12):1123-31.
42. Peluso D, Badano LP, Muraru D, Dal Bianco L, Cucchini U, Kocabay G, et al. Right atrial size and function assessed with three-dimensional and speckle-tracking echocardiography in 200 healthy volunteers. *Eur Heart J Cardiovasc Imaging*. 2013;14(11):1106-14.
43. Nemes A, Domsik P, Kalapos A, Forster T. Three-dimensional strain analysis of the popliteal artery by three-dimensional speckle-tracking echocardiography (from the MAGYAR-Healthy Study). *Int J Cardiol*. 2016;223:290-1.
44. Nesser HJ, Mor-Avi V, Gorissen W, Weinert L, Steringer-Mascherbauer R, Niel J, et al. Quantification of left ventricular volumes using three-dimensional echocardiographic speckle tracking: comparison with MRI. *Eur Heart J*. 2009;30(13):1565-73.
45. Kleijn SA, Brouwer WP, Aly MF, Russel IK, de Roest GJ, Beek AM, et al. Comparison between three-dimensional speckle-tracking echocardiography and cardiac magnetic resonance imaging for quantification of left ventricular volumes and function. *Eur Heart J Cardiovasc Imaging*. 2012;13(10):834-9.

46. Kleijn SA, Aly MF, Terwee CB, van Rossum AC, Kamp O. Reliability of left ventricular volumes and function measurements using three-dimensional speckle tracking echocardiography. *Eur Heart J Cardiovasc Imaging*. 2012;13(2):159-68.
47. Kleijn SA, Aly MF, Terwee CB, van Rossum AC, Kamp O. Comparison between direct volumetric and speckle tracking methodologies for left ventricular and left atrial chamber quantification by three-dimensional echocardiography. *Am J Cardiol*. 2011;108(7):1038-44.
48. Saito K, Okura H, Watanabe N, Hayashida A, Obase K, Imai K, et al. Comprehensive evaluation of left ventricular strain using speckle tracking echocardiography in normal adults: comparison of three-dimensional and two-dimensional approaches. *J Am Soc Echocardiogr*. 2009;22(9):1025-30.
49. Seo Y, Ishizu T, Enomoto Y, Sugimori H, Yamamoto M, Machino T, et al. Validation of 3-dimensional speckle tracking imaging to quantify regional myocardial deformation. *Circ Cardiovasc Imaging*. 2009;2(6):451-9.
50. Maffessanti F, Nesser HJ, Weinert L, Steringer-Mascherbauer R, Niel J, Gorissen W, et al. Quantitative evaluation of regional left ventricular function using three-dimensional speckle tracking echocardiography in patients with and without heart disease. *Am J Cardiol*. 2009;104(12):1755-62.
51. Mochizuki A, Yuda S, Oi Y, Kawamukai M, Nishida J, Kouzu H, et al. Assessment of left atrial deformation and synchrony by three-dimensional speckle-tracking echocardiography: comparative studies in healthy subjects and patients with atrial fibrillation. *J Am Soc Echocardiogr*. 2013;26(2):165-74.
52. Tanaka H, Hara H, Saba S, Gorcsan J, 3rd. Usefulness of three-dimensional speckle tracking strain to quantify dyssynchrony and the site of latest mechanical activation. *Am J Cardiol*. 2010;105(2):235-42.
53. Li CH, Carreras F, Leta R, Carballeira L, Pujadas S, Pons-Llado G. Mechanical left ventricular dyssynchrony detection by endocardium displacement analysis with 3D speckle tracking technology. *Int J Cardiovasc Imaging*. 2010;26(8):867-70.
54. Tatsumi K, Tanaka H, Tsuji T, Kaneko A, Ryo K, Yamawaki K, et al. Strain dyssynchrony index determined by three-dimensional speckle area tracking can predict response to cardiac resynchronization therapy. *Cardiovasc Ultrasound*. 2011;9:11.
55. Riesenkampff E, Al-Wakeel N, Kropf S, Stamm C, Alexi-Meskishvili V, Berger F, et al. Surgery impacts right atrial function in tetralogy of Fallot. *J Thorac Cardiovasc Surg*. 2014;147(4):1306-11.

56. Nemes A, Domsik P, Kalapos A, Gavaller H, Oszlanczi M, Forster T. Right atrial deformation analysis in isolated left ventricular noncompaction - insights from the three-dimensional speckle tracking echocardiographic MAGYAR-Path Study. *Rev Port Cardiol.* 2016;35(10):515-21.
57. Menting ME, Eindhoven JA, van den Bosch AE, Cuypers JA, Ruys TP, van Dalen BM, et al. Abnormal left ventricular rotation and twist in adult patients with corrected tetralogy of Fallot. *Eur Heart J Cardiovasc Imaging.* 2014;15(5):566-74.
58. Roos-Hesselink J, Perlroth MG, McGhie J, Spitaels S. Atrial arrhythmias in adults after repair of tetralogy of Fallot. Correlations with clinical, exercise, and echocardiographic findings. *Circulation.* 1995;91(8):2214-9.
59. Peters F, Khandheria BK, Libhaber E, Maharaj N, Dos Santos C, Matioda H, et al. Left ventricular twist in left ventricular noncompaction. *Eur Heart J Cardiovasc Imaging.* 2014;15(1):48-55.
60. Kalapos A, Domsik P, Forster T, Nemes A. [Comparative evaluation of left ventricular function by two-dimensional echocardiography and three-dimensional speckle-tracking echocardiography in noncompaction cardiomyopathy. Results from the MAGYAR-Path Study]. *Orv Hetil.* 2013;154(34):1352-9.
61. Truong UT, Li X, Broberg CS, Houle H, Schaal M, Ashraf M, et al. Significance of mechanical alterations in single ventricle patients on twisting and circumferential strain as determined by analysis of strain from gradient cine magnetic resonance imaging sequences. *Am J Cardiol.* 2010;105(10):1465-9.
62. Zhou Z, Ashraf M, Hu D, Dai X, Xu Y, Kenny B, et al. Three-dimensional speckle-tracking imaging for left ventricular rotation measurement: an in vitro validation study. *J Ultrasound Med.* 2010;29(6):903-9.

8. Acknowledgements

The studies reported in this work were performed at the 2nd Department of Medicine and Cardiology Center, Medical Faculty, Albert Szent-Györgyi Clinical Center, University of Szeged, Hungary.

First of all, I express my heartfelt gratitude to Prof. Dr. Attila Nemes for his continuous support during my work, who was my tutor and scientific adviser. Without his support and encouragement, this thesis would have not been performed.

I would like to thank very much also Prof. Dr. Tamás Forster, the head of the 2nd Department of Medicine and Cardiology Center, who supported me in my work.

I would like to thank all co-authors, Dr. Péter Domsik, Dr. Anita Kalapos, Dr. Kriszinta Berek, Dr. Mária Kohári, Dr. Gábor Bogáts, Prof. Dr. Gábor Kovács, Prof. Dr. István Hartyánszky, Jackie S. McGhie, Prof. Dr. Jolien W. Roos-Hesselink.

I thank all my colleagues as well as nurses, assistants and all the members of the Institute.

Photocopies of essential publications